DETECTION & PARAMETER ESTIMATION OF FREQUENCY HOPPING (FH) SIGNAL

By

Saira Anwar

Submitted to the Faculty of Electrical Engineering

Military College of Signals (NUST), Rawalpindi

In partial fulfillment for the requirements of MS (Telecom) Degree in

Electrical Engineering

MARCH 2016

ABSTRACT

The thesis is based on the detection and characterization of frequency hopping (FH) signals, operating in HF (2-30MHz) band. The work is focused on the blind detection and parameter estimation of FH. The algorithm does not require any prior information about the hop frequencies, hop pattern or modulation type. For reception of a frequency hopping signal, the first step is detection of the signal. Detection & Estimation Algorithm, presented in this thesis, detects the presence of hop and estimates the time of hop. The detection technique used in this work is wavelet based transient detection. Discontinuities are enhanced via wavelet transform. For the hop time estimation of frequency hopping signal, firstly, the phase information is extracted from the temporal correlation function (TCF) of received signal. Then, by applying certain de-noising techniques, discrete wavelet transform (DWT) is used for extracting the time of hopping.

Simulations are carried out in MATLAB with Additive White Gaussian (AWGN) Channel and the results are presented in the form of detection statistics. Results show reliable detection and estimation performance for SNR levels above 3dB.

DEDICATION

I would dedicate this thesis to my beloved father, Khawaja Anwar-Ul-Haq (Late)

ACKNOWLEDGEMENT

I am very thankful to the almighty, the most merciful, Allah for giving me the ability and strength to work on this thesis. I would like to thank my advisor, Dr Adnan Ahmed Khan, whose guidance and support made it possible. It has been a pleasure to work with and learn from him. His helpful comments guided me a lot. I would also express my sincere gratitude to Dr Imran Touqeer for his superb technical support, motivation and encouragement throughout my thesis. I would also thank my colleagues for their help and moral support.

I would extend my thanks to my mother for her steady encouragement and prayers throughout my graduate studies. Special thanks to my husband for his moral support and for believing in me.

TABLE OF CONTENTS

LIST OF TABLES

LI ST OF FIGURES

LIST OF ACRONYMS

FHSS	Frequency Hopping Spread Spectrum
FSK	Frequency Shift Keying
MFSK	Multiple-Frequency Shift Keying
SFH	Slow Frequency Hopping
FFH	Fast Frequency Hopping
TCF	Temporal Correlation Function
FT	Fourier Transform
STFT	Short Time Fourier Transform
MRA	Multi-resolution Analysis
WT	Wavelet Transform
CWT	Continuous Wavelet Transform
DWT	Discrete Wavelet Transform

THIS PAGE INTENTIONALLY LEFT BLANK

Chapter 1

INTRODUCTION

This chapter provides an introduction of the research topic along with the defining features of the technology. It introduces the concept of Frequency Hopping Spread Spectrum and its detection techniques. The problem statement is provided to explain the work done in this thesis. Organization of the report is also clearly outlined in the chapter.

1.1 Concept of Frequency Hopping Spread Spectrum

Frequency hopping spread spectrum (FHSS) is a wireless communication technique in which the signal's bandwidth is distributed over a much larger bandwidth (spread bandwidth) by hopping the carrier frequency.

The information or data signal in FHSS is a lesser bandwidth signal and the data signal is generally FSK modulated. This modulated signal "hops" randomly in frequency and hopping is carried out in a pseudo-random "predictable" format with respect to time from frequency to another. Using FHSS improves privacy, rejects unintended interference and multi-path fading (distortion), it enhances signal capacity and improves the signal to noise ratio.

In FH systems the available bandwidth, W is subdivided into a large number of frequency slots, N. The data symbol modulates the carrier frequency, f_k, where k is selected by a pseudorandom number (PN) generator to be between 1 and N.

The FH system can be thought of as a two-step modulation process. The first step MFSK modulation would be followed by the second step, FH modulation.

Pattern of transmitted signal in the time-frequency plane will be affected primarily by the FH modulation step, regardless of the particular modulation scheme or the number of symbols transmitted per hop. For a given hop, the occupied bandwidth is the same as that for conventional MFSK. When considered over many hops a much greater bandwidth equal to W is occupied, and the spectrum has been spread.

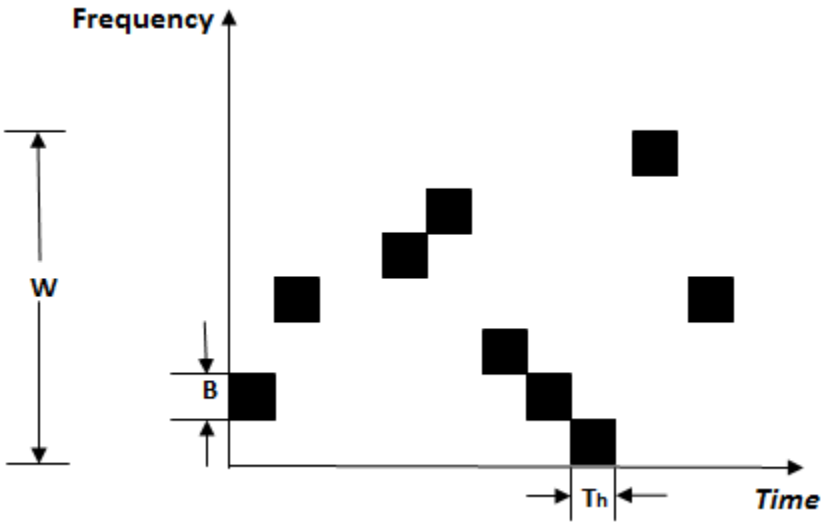

Figure 1.1 Frequency Hopping Spread Spectrum in Time-Frequency Plane [5]

FHSS is characterized as slow frequency hopping (SFH) and fast frequency hopping (FFH). In SFH hop rate is slow and numerous symbols are transmitted in a single hop. On the other hand, in FFH hop rate is fast and the carrier frequency hops a number of times during the transmission of a single symbol.

1.1.1 Advantages

In FHSS, the information signal's spectrum is distributed over a much wider bandwidth than that of the original signal. An intentional jammer has a fixed finite power. The jammer may either spread its power in small quantities over the entire spread bandwidth

or it may concentrate its power on any part of the spread bandwidth. In the first case, the jammer's power being spread over a wide bandwidth would not be able to jam the FHSS signal. In the other case, FHSS signal would reduce the interference since it will not occupy the same spectral location as the jammer for the entire transmission. Thus, FHSS has the characteristic of anti-jamming or interference suppression.

A spread spectrum technique has a Low Probability of Interception. This is because the signal's power is distributed over a wider spread bandwidth, its strength at any given frequency wouldn't be significant to be intercepted. Moreover, FHSS signal cannot be intercepted without prior knowledge of the frequency hop sequence. Hence it can be said that FHSS provides secure communication.

Due to the underlying benefits of FHSS, it has found widespread applications in wireless communication technology.

1.2 Literature Review

Various techniques have been used in literature for the detection, characterization and demodulaion of Frequency Hopping Signals. These include energy detection technique, maximum likelihood approach, auto-correlation based detection, polyphase filter banks, wavelet detection and many of their variants. A comparison of few techniques is given in [1]. Energy detection is not robust to noise and its detection performance degrades at low SNR. Energy Detection technique gives a coarse estimate about the availability of a signal's energy by measuring the energy of the signal and comparing it against a threshold. Maximum Likelihood detector has very good performance but it requires prior knowledge of the FH signal so it cannot be used for non-cooperative detection. The use

of polyphase filter banks using Fast Fourier Transform (FFT) was presented in [2]. Parameter characterization of Frequency Hopping Signal incorporate determination of its time of hop, hop frequencies, hop sequence and hop rate. Various techniques have been applied for estimation of these parameters [3], [4]. In [6], [7] and [12] wavelet transform of temporal correlation function is used for detection and for extracting the time of hop. In [13], [14] and [15], compressive sensing is used for the detection of wideband Frequency Hopping signals in the Industrial, Scientific and Medical (ISM) band.

HF (2 – 30MHz) band is specifically used for military communications. The main goal of this thesis is to work on FH Signal in HF band. "Wavelet Analysis" is best suited technique for this frequency band that is why DWT is used in this thesis for the detection and hop time evaluation, so as to get good Detection Performance and accurate Hop Time Estimation of FHSS signal.

FHSS signal consists of both, low frequency constituents (carrier frequencies) for a relatively long time interval and transitional high frequency constituents (frequency hops) for a small time interval. This implies that Multi-Resolution Analysis will be a good technique to be used for FHSS signals. Wavelet Analysis has Multi-resolution capabilities. It enables one to "zoom in" to have a detailed view and "zoom out" to have an overall global view of the signal.

1.3 Problem Statement

Research is carried out to blindly detect a Frequency Hopping Signal in HF band. In case a hop is detected, its hop time is estimated.

The technique used in this work is Discrete Haar Wavelet Transform. The methodology involved does not require any prior information about the hop frequencies, hop pattern or

modulation type. In the detection phase, the frequency hopping properties (as apparent in the Time-Frequency representation) of the signal are important irrespective of the modulation scheme involved or the number of symbols transmitted per hop.

1.4 Organization of Thesis

This thesis has six chapters including the first chapter of introduction. Chapter 2 gives an idea about the Temporal Correlation Function (TCF). Phase plot of TCF forms the basis of the detection and estimation of FH signal. The chapter explains how the two-dimensional phase plot of TCF can be used to detect and estimate the hop time of FH signal. It further discusses the pre-processing methods necessary before applying the Wavelet Analysis. Chapter 3 explains the basics of Wavelet Analysis as a useful Multi-resolution Analysis Technique required for the study of non-stationary signals. Chapter also provides the application of Wavelet Transform in transient detection. Chapter 5 discusses the steps of the Algorithm for Detection & Hop Time Estimation of FH signal in the HF band. It also gives detail about the MATLAB simulations carried out for testing the algorithm. Lastly, chapter 6 provides the conclusions and proposed future work.

Chapter 2

TEMPORAL CORRELATION FUNCTION

This Chapter gives an idea about the Temporal Correlation Function (TCF), its mathematical interpretation and phase plot. Phase plot of TCF forms the basis of the detection and estimation of FH signal. The chapter explains how the two- dimensional phase plot of TCF can be used to detect and estimate the hop time of FH signal. Later in this chapter, few pre-processing techniques are explained which are necessary for eliminating the effect of noise from the TCF phase plot.

2.1 Definition

Temporal Correlation Function provides time correlation of a signal. It is used for non-stationary signals. Mathematically, TCF of a signal y(t) is expressed as [6]

$$TCF(t,\tau) = y(t+\tau)y^*(t-\tau) \quad 2.1$$

Where,'t' corresponds to time, 'τ' is the lag time and * is the complex conjugate.

Along the τ- axis, TCF is conjugate symmetric i.e.

$$TCF(t,\tau) = TCF^*(t,-\tau) \quad 2.2$$

It means that TCF along negative τ-axis gives no additional information.

2.2 TCF of a Real Signal versus an Analytic Signal

Let *x(t)* be a real sinusoidal signal, expressed as:

$$x(t) = \sin(2\pi ft + \theta) \quad 2.3$$

TCF of *x(t)* will be:

$$TCF(t,\tau) = \tfrac{1}{2}[\cos(2\pi ft) - \cos(2\pi(2f)t + 2\theta)] \quad 2.4$$

The first term in brackets is the auto-term at frequency, f and the second term is at twice the frequency of x(t).

An Analytical Signal has no negative frequency components. It facilitates many mathematical calculations. The analytic form of the signal is used as a substitute for its real expression when it is required to suppress cross interference. While performing time-frequency analysis, real signals result in more cross interference as compared to the analytic form of signals. Moreover, on removing the negative frequency components, there is no loss of data as well. Before time frequency analysis a real data signal is converted to its respective analytic form by using Hilbert Transform.

If we consider the Analytical Signal, $x_a(t)$ derived from x(t), given as:

$$x_a(t) = e^{j2\pi f t+\theta} \quad 2.5$$

In this case TCF will be:

$$TCF(t,\tau) = e^{j2\pi f \tau} \quad 2.6$$

It is clear from equation 2.6 that the expression for TCF now contains only the auto-term at frequency of $x_a(t)$, i.e. there are no interference terms that would have been present if real form of signal x(t) was considered instead of its transformed analytical form.

It is for this reason that Analytical Form of the frequency hopping signal is considered in this thesis for Time-Frequency Analysis.

2.3 TCF of Frequency Hopping Signal

Mathematically, the analytic expression of frequency hopping signal is given as [6]:

$$x_a(t) = e^{j2\pi f_1 t}\left[u(t) - u\left(t - T_{hop}\right)\right] + e^{j2\pi f_2 t}\left[u\left(t - T_{hop} + 1\right) - u(t - T)\right] \quad 2.7$$

for $0 \leq t \leq T$,

T_{hop} is the time of hop of the signal from one frequency f_1 to f_2.

u(t) is a unit step function defined as:

$$u(t) = \begin{cases} 1, & for\ t\ \geq 0 \\ 0, & for\ t\ \leq 0 \end{cases}$$

Now putting equation 2.7 in equation 2.1 gives the expression for TCF as:

$$TCF(t,\tau) = e^{j2\pi(2f_1)\tau}\left[u(t-\tau) - u\left(t+\tau-T_{hop}\right)\right]\left[u(t-\tau) - u\left(t-\tau-T_{hop}\right)\right] +$$

$$e^{j2\pi(2f_2)\tau}\left[u\left(t+\tau-T_{hop}+1\right) - u(t+\tau-T)\right]\left[u\left(t-\tau-T_{hop}+1\right) - u(t-\tau-T)\right]$$

$$+e^{j2\pi[(f_2-f_1)t+(f_1+f_2)\tau]}\left[u(t+\tau) - u\left(t+\tau-T_{hop}\right)\right]\left[u\left(t-\tau-T_{hop}+1\right) -\right.$$

$$\left.u(t-\tau-T)\right] + \left[u(t-\tau) - u\left(t-\tau-T_{hop}\right)\right][u\left(t+\tau-T_{hop}+1\right) - u(t+\tau-T)] \quad 2.8$$

Equation 2.8 can also be understood in a simplified manner as:

$$TCF(t, \tau) = TCF_1(t, \tau) + TCF_2(t, \tau) + TCF_{12}(t, \tau) \quad 2.9$$

The three terms given in Equation 2.8, appear as non-overlapping triangular shaped regions which constitute the complete TCF expression. The unit step functions are used to model the boundary lines between the three triangular shaped $TCF_1(t, \tau)$, $TCF_2(t, \tau)$ and $TCF_{12}(t, \tau)$ phase regions. These triangular regions have an orientation of 45°. $TCF_1(t, \tau)$ and $TCF_2(t, \tau)$ may be called the auto-term triangle and $TCF_{12}(t, \tau)$ as cross-term triangular region.

The phase of $TCF_1(t, \tau)$ and $TCF_2(t, \tau)$ are $2\pi f_1\tau$ and $2\pi f_2\tau$ respectively and are constant with respect to the variable 't'. $TCF_1(t, \tau)$ depends on f_1 and τ. Similarly, $TCF_2(t, \tau)$ depends on f_2 and τ . It means that for a given value of frequency and lag, $TCF_1(t, \tau)$ shows a constant phase. Same is the case for $TCF_2(t, \tau)$. The phase of $TCF_{12}(t, \tau)$ depends on f_1, f_2, time (t) and lag (τ). Thus for a fixed value of τ, TCF phase expressed as a function of 't' undergoes changes in its slope value when going from one region to another one. Moreover, cross-terms region exhibits a linear phase response.

Figure 2.1 shows the TCF phase plot for the signal $x_a(t)$, given by Equation 2.7, for $\mathbf{f_1}$=25.89 MHz, $\mathbf{f_2}$=24.2 MHz and $\mathbf{T_h}$= 139 samples. It is clear from figure that T_{hop} is the time at which the triangular region covered by $TCF_1(t, \tau)$ ends and the triangular region covered by $TCF_2(t, \tau)$ starts.

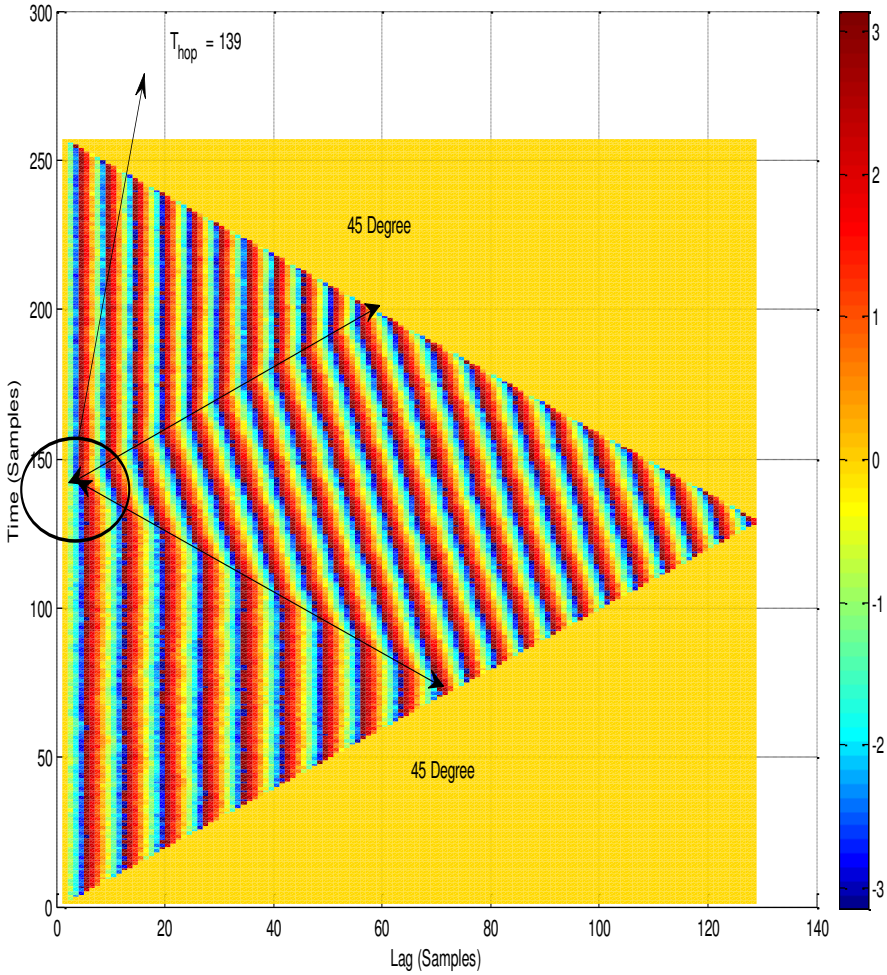

Figure 2.1 TCF Phase Plot

Across $TCF_{12}(t,\tau)$, the phase behavior is periodic over 2π producing discontinuities at regular intervals. The period of these intervals is a function of f_1 and f_2 and, therefore, not predictable without knowing f_1 and f_2. As far as the lag, $\tau < T_{hop}$, the cross-terms region is

centered on the hopping instant, T_{hop}**.** Within a given auto-term triangle, there is only one frequency component across the τ-axis.

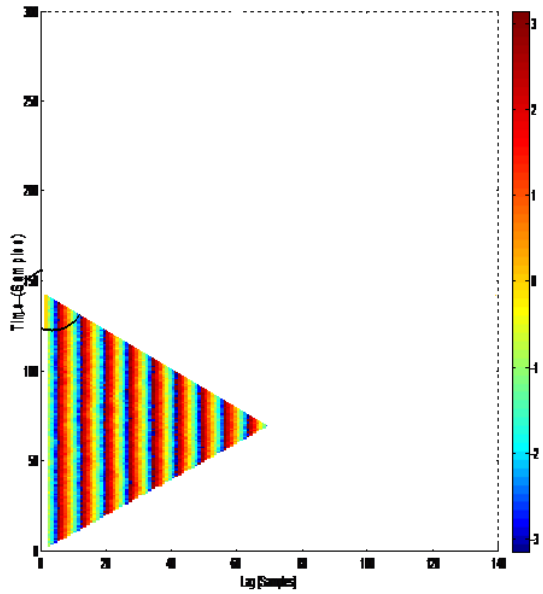

Figure 2.2 Portion of the Phase plot of TCF, containing auto-term TCF_1 due to f_1

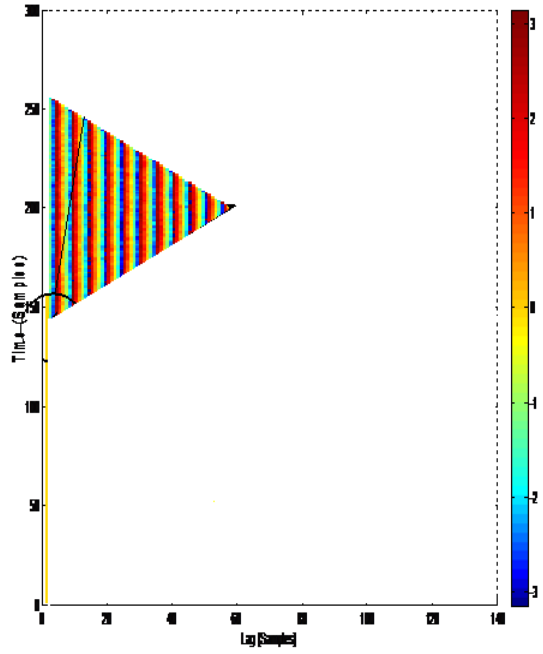

Figure 2.3 Portion of the Phase plot of TCF, containing auto-term TCF_2 due to f_2

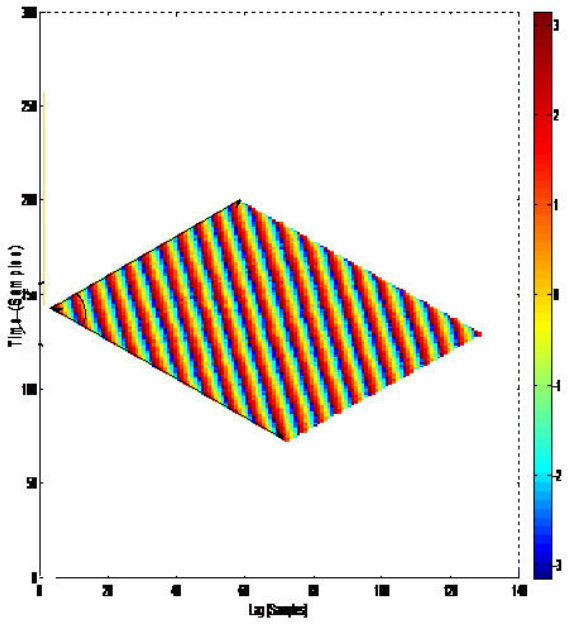

Figure 2.4 Portion of the Phase plot of TCF given in Figure 2.1, containing cross-term TCF_{12} due to both f_1 and f_1

2.4 Pre-processing Techniques

Till now, a noise-free signal has been considered but in practice it is not possible to have a noise-free signal. The detection process actually relies on changes observed between the three TCF phase regions discussed in the previous section. Hop time location estimation degrades significantly with increasing noise levels. Figure 2.5 shows an example demonstrating the effect of Additive White Gaussian Noise (AWGN) on TCF phase as a function of time, with SNR of 10 dB and a lag, $\tau = 25$. It can be observed from the figure that $TCF_1(t, \tau)$ and $TCF_2(t, \tau)$ are no more constant with respect to time. Noise distortion introduces random spikes in phase. A reliable detection algorithm must minimize such spike occurrences. Similarly the phase region in $TCF_{12}(t, \tau)$ region is also not linear. It is now very difficult to detect discontinuities in frequency hopping signal

and also to extract the hop time in the presence of noise. It is therefore necessary to apply some de-nosing or pre-processing techniques before applying the Wavelet Transform.

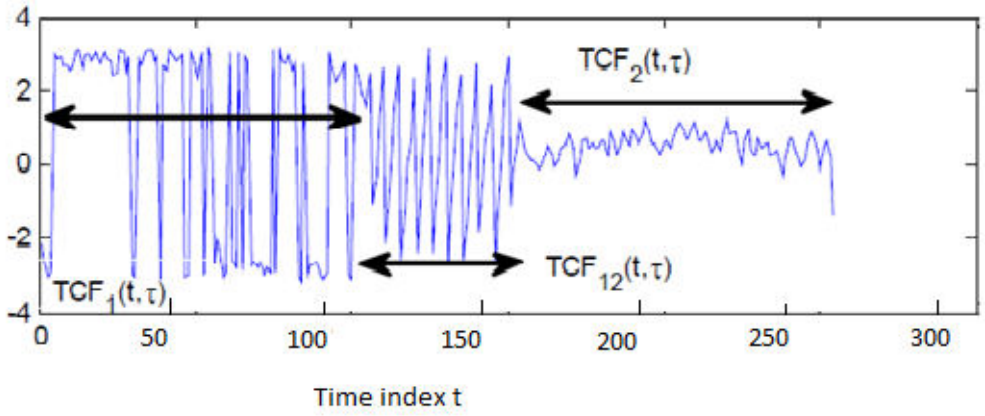

Figure 2.5 TCF Phase at SNR=9dB, τ = 25 subjected to AWGN[6]

The following three pre-processing techniques are used in this work for de-noising.

2.4.1 Phase Unwrapping

Phase unwrapping transforms jumps greater than π between successive points to their 2π complement. It ensures that all the suitable multiples of 2π have been included in the phase response. Phase unwrapping eliminate the discontinuities due to periodicity in phase and reduces the spikes due to noise.

Mathematically, TCF phase φ(t) of a signal y(t) can be unwrapped as [7]:

$$\text{Unwrap } (\varphi(t)) = \begin{cases} \varphi(t), & if\ |\varphi(t) - \varphi(t-1)| \leq \pi \\ \varphi(t) + 2\pi & if\ \varphi(t) - \varphi(t-1) < -\pi \\ \varphi(t) - 2\pi & if\ \varphi(t) - \varphi(t-1) > \pi \end{cases} \quad 2.10$$

Figure 2.6 describes the results obtained by unwrapping the TCF phase function with respect to the time axis (for a value of τ =25). Observe that the phase behavior for times between [0 120] and [160 256]. These portions correspond to the TCF_1 and TCF_2 regions

where the phase should have been theoretically constant for a noise free signal (as a function of t, for a fixed value of τ). But due to presence of noise, TCF_1 and TCF_2 regions exhibit sudden phase jumps. The phase behavior in the TCF_{12} region [120 160] should ideally be linear (as a function of t, for a fixed value of τ). But due to noise multiple phase jumps are observed in TCF_{12} region.

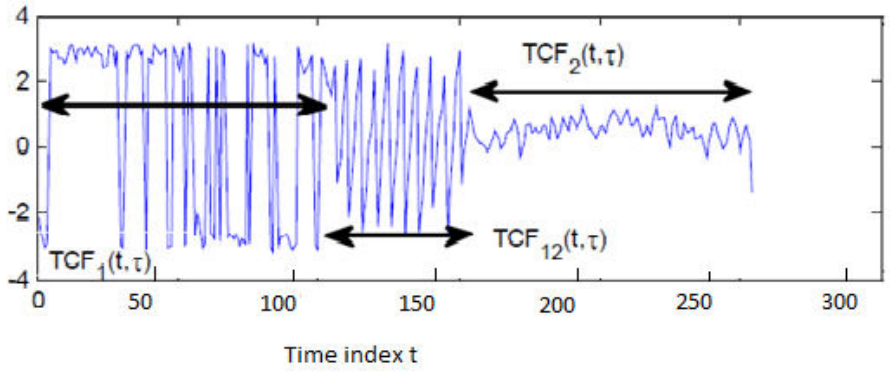

(a)

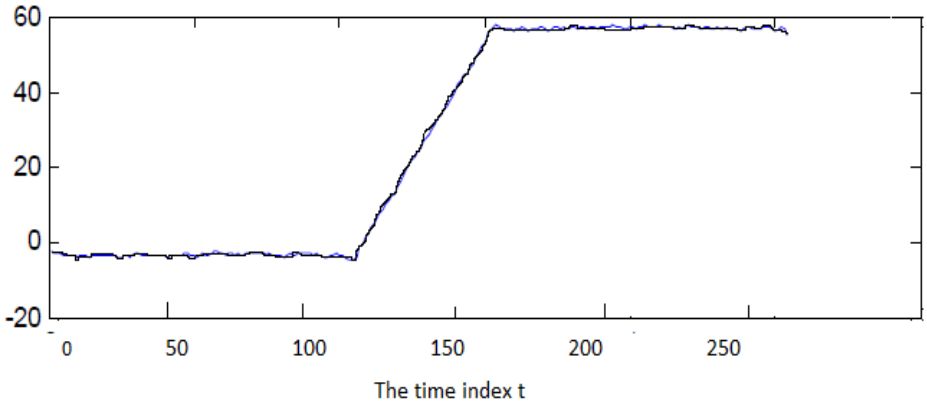

s(b)

Figure 2.6 TCF Phase plotted as a function of time at SNR=9dB and τ=25, (a) before unwrapping and (b) after unwrapping

After unwrapping the TCF phase, phase behavior in TCF_1 and TCF_2 regions becomes almost constant with very small phase variations and phase in TCF_{12} also becomes linear. It can also be observed from the plot that there is large gap in phase value between TCF_1 and TCF_2 regions.

2.4.2 Differentiation

As discussed in the previous section, TCF phase graphically shown as a function of time with a fixed value of lag (τ) has three portions. TCF_1 and TCF_2 regions have almost flat lines while TCF_{12} region shows a ramp. In other words, there are two discontinuities in the phase plot on the whole. Differentiation sharpens these discontinuities.

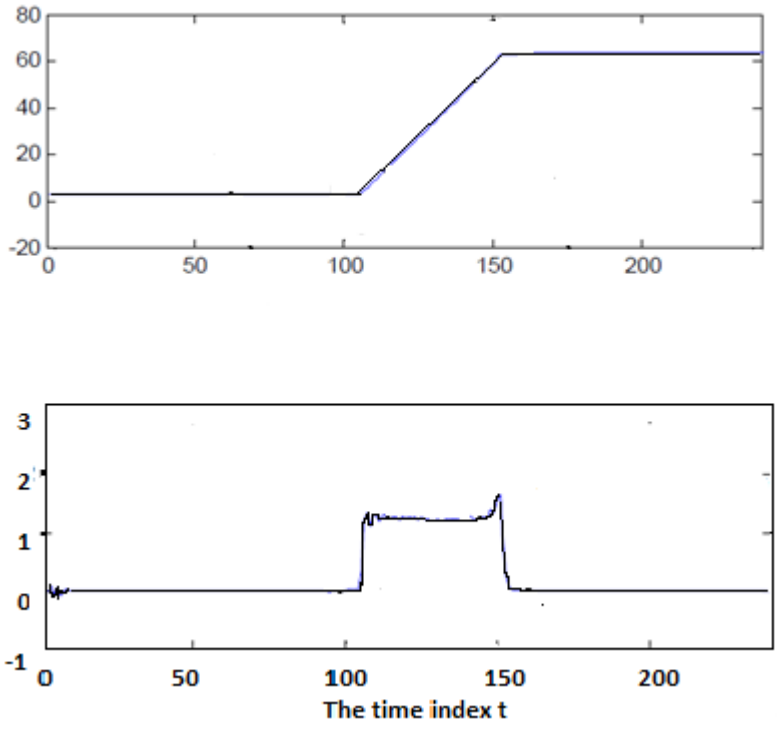

Figure 2.7 Unwrapped TCF Phase plot (top), TCF Phase plot after Differentiation [6]

The first derivative of a constant is zero and that of a ramp is a constant whose value is equal to the slope of the ramp, which is determined as

$$\text{Slope} = \frac{y_2 - y_1}{t_2 - t_1} = \frac{\Delta\, amplitude}{\Delta\, time} \qquad 2.11$$

Figure 2.7 depicts the result obtained by applying differentiation to the unwrapped TCF Phase plot. When the unwrapped phase is differentiated with respect to time, we get a pulse for the ramp portion and zero otherwise. It is important to notice that this pulse is centered on the hop time, T_{hop}, for $\tau < T_{hop}$.

Differentiation is followed by another de-noising technique, known as Median Filtering. Median Filtering smoothes out the noise contribution, as discussed in the next section.

2.4.3 Median Filtering

Median Filter is a non-linear digital filter employed for the suppression of impulse errors or short-term discontinuities superimposed on an image or a signal. It is used as a preliminary step that improves the results of later processing. Median filtering is extensively used in digital image processing because it has the ability to remove noise whilst preserving edges. An important feature of median filter is that it does not average out and hence preserves edges.

In a median filter, the basic concept is to slip a window through the signal's samples one by one, substituting each sample value by the median of adjacent sample values. For one-dimensional signals, the window contains only a few entries, while for two-dimensional (or higher-dimensional) signals such as images, little more complicated window formats such as "box" or "cross" patterns can be used. When the window size is odd, then after numerically arranging all the sample values, median is merely taken as the centre value.

For a vector of values, f(n) given as:

$$f(n) = \{f(n), f(n-1), f(n-2),\ldots, f(n-M)\}^T \quad 2.12$$

Here M is an arbitrary positive integer

Median filter's output, z(n) is defined as [8] middle sample of the collection of elements of x(n)

$$z(n) = \text{med}\{x(i)\} \quad 2.13$$

for i = n, n-1, n-2, …., n-M

Number of samples of M+1 median filter is known as length D of it. Length of median filter is usually odd and it determines suppression of impulse errors with various widths.

After performing phase unwrapping, differentiation and median filtering of the TCF phase plot, wavelet transform is applied for the detection of frequency hop and its hop time evaluation. The following chapter provides the details of wavelet transform and its underlying concepts.

Chapter 3

WAVELET ANALYSIS

It has been shown in Chapter 2 that the TCF plot has three phase regions and after applying the pre-processing techniques at a fixed value of lag, a pulse-shaped TCF phase plot is obtained. Thus the phase plot exhibits step discontinuities at the TCF_{12} cross-term region. This chapter provides the concepts of signal processing, starting from Fourier Transform to Discrete Wavelet Transform. It explains how wavelet transform is capable of detecting the step discontinuities at the TCF_{12} cross-term region (caused by frequency transition).

3.1 Fourier Transform (FT)

Frequency Transform of a signal shows the frequency constituents (spectral components) that make up the signal. It is depicted as a frequency spectrum which is called frequency-domain or frequency-amplitude representation of the signal. A frequency spectrum shows how much of each frequency is present in a signal. Fourier transform is a tool used for frequency analysis of a signal.

Fourier transform converts a time-domain signal into frequency-domain. Mathematically, transformation can be represented as [5]:

$$x(f) = \int_{-\infty}^{+\infty} x(t) e^{-2\pi f t} dt \qquad 3.1$$

Fourier Transform tells about the frequency components of the signal but it does not show **at what time** these frequency components will be present. No time information is obtained from the frequency transform of a signal. For this reason, frequency analysis is well suited for stationary signals. Frequency contents of stationary signals have no

variation with respect to time i.e. all frequency components are present at all times. It is not used in this thesis because in a Frequency Hopping Spread Spectrum signal, the frequency components of the signal change with time. Such signals are called non-stationary signals. For the study of non-stationary signals, time localization of spectral components is also essential, so a transform providing the Time-Frequency representation of signal is desired.

Figure 3.1 shows different signal processing techniques used for stationary and non-stationary signals.

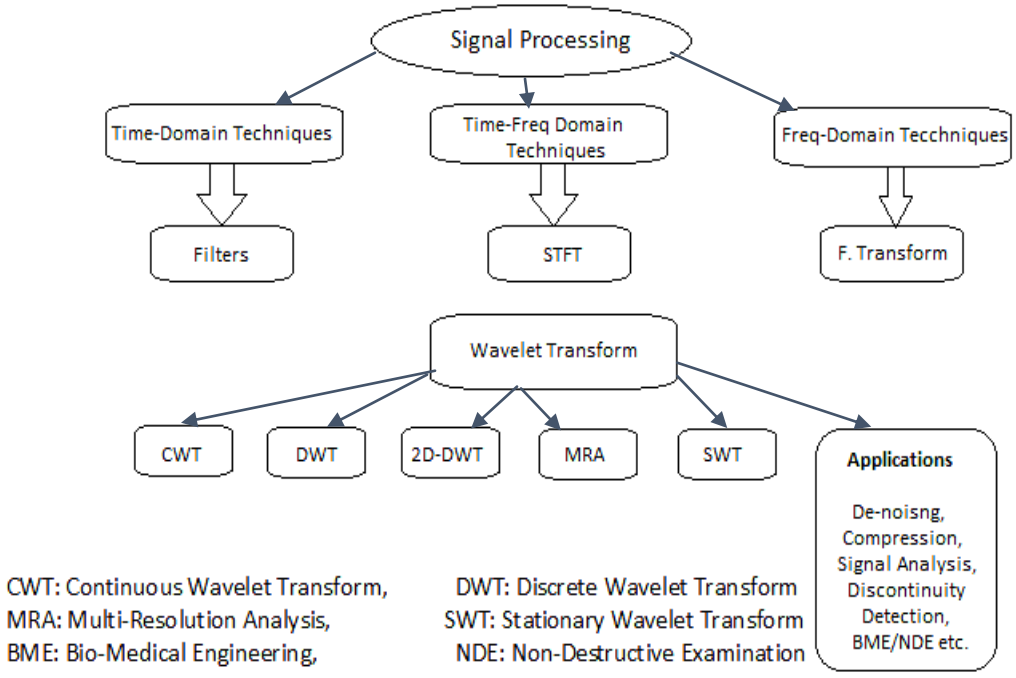

Figure 3.1 Signal Processing Techniques

3.2 Short Time Fourier Transform (STFT)

Short-Time Fourier Transform provides both time-based and frequency-based representations of the non-stationary signal. It gives a Time-Frequency representation of the signal. STFT provides the time information by computing a different FT for

successive time intervals, and then putting them together. It may be called windowed FT. The signal is segmented into narrow time intervals (i.e., narrow enough to be considered stationary) and then Fourier transform of each segment is determined. A different FT is obtained when the window is centered at each time location. Each FT provides the frequency content of a separate time-slot of the signal, thereby providing both time and frequency representation, at the same time.

Mathematically, STFT can be represented as [5]:

$$STFT(\tau, f) = \int x(t) g^*(t-\tau) e^{-j2\pi f t} dt \qquad 3.2$$

Here $g^*(t-\tau)$ represents the finite time sliding windowing function that is centered on τ. Length of the window is selected in such a way that the signal can be considered stationary in that interval. Window length determines the time and frequency resolutions. A wide analysis window gives poor time resolution and good frequency resolution while a narrow analysis window provides good time resolution and poor frequency resolution. Once the window is chosen, the resolution is set for both time and frequency.

For the extreme case of an infinitely long window, i.e. g(t) = 1, STFT becomes FT, providing excellent frequency information but no time information. For the case of infinitely short window, i.e. g(t) = δ(t), STFT gives the time signal back, with a phase factor, providing excellent time localization but no frequency information. According to Heisenberg Uncertainty Principle, both frequency and time resolutions cannot be arbitrarily high. It can also be depicted as

$$\Delta f . \Delta t \geq 1/4\pi \qquad 3.3$$

Frequency resolution, Δf, determines how well two spectral components can be separated from each other in the transform domain and Time resolution, Δt, determines how well two spikes in time can be separated from each other in the transform domain.

A major drawback of STFT is that the window once chosen remains fixed for all the bandwidth. Many non-stationary signals have both the long duration components as well the transient components. Analysis of such signals requires flexibility in the choice of window size for different parts of the spectrum so as to obtain more accurate either time or frequency localization. STFT is therefore not suited for this thesis because FHSS signals require a multi-resolution analysis technique for accurate hop tome estimation.

3.3 Wavelet Transform

Wavelet transform (WT) is a multi-resolution analysis technique. Unlike STFT, it has variable time-frequency resolution. This characteristic makes it a good choice for analyzing non-stationary signals having sudden discontinuities, as the discontinuities in the TCF phase plot discussed in the previous chapter.

Wavelet Transform analyzes the signal at different frequencies with different resolutions. High frequencies have good time resolution and low frequencies have good frequency resolution. It is beneficial as it allows the low frequency components, which usually characterize or identify a signal, to be distinguished from one another in terms of their frequency content, while providing an excellent temporal resolution for the high frequency components, sudden discontinuities or frequency hops of signal. Hence it is more suitable for short duration of higher frequency and longer duration of lower frequency components.

Figure 3.2 shows a comparison of Time-Frequency plane tiling for Fourier Transform and Wavelet Transform.

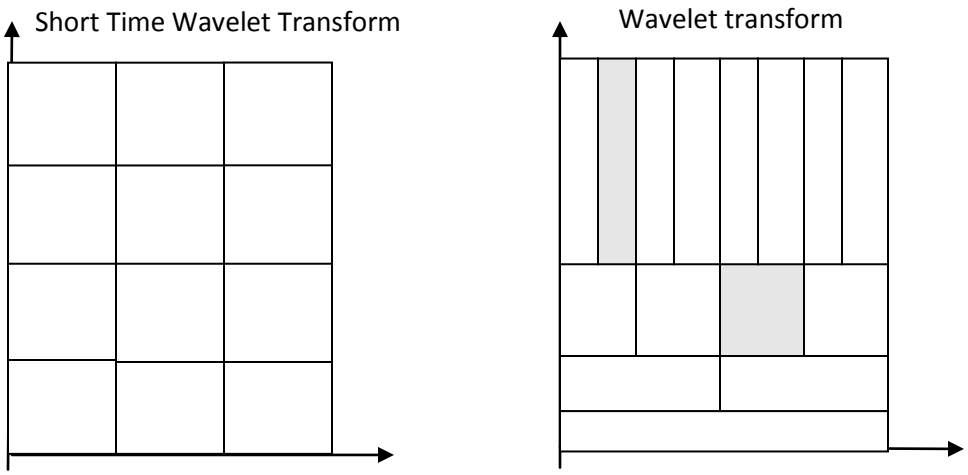

Figure 3.2 Time-Frequency Plane Resolution for STFT and WT

3.4 Continuous Wavelet Transform

The wavelet transform is a tool for representing functions, signal, or data into components of different frequency, allowing one to study each component separately.

The word "wavelet" means a "small wave". Wavelet is defined over a finite interval and has an average value of zero.

Mathematically, a wavelet can be interpreted as:

$$\int_{-\infty}^{\infty} \psi(t)dt = 0 \qquad 3.4$$

and

$$\int_{-\infty}^{\infty} |\psi(t)|^2 < \infty \qquad 3.5$$

Equation 3.4 implies that wavelet is an oscillation having an average value of zero and hence it is compactly supported. Equation 3.5 implies that the wavelet which is defined over a finite interval has a finite energy.

Wavelet transform basically represents any function as a superposition of a set of wavelets or basis functions. The basis functions or baby wavelets are derived from a

single prototype wavelet called the mother wavelet, by scaling (expansion or compression) and translations (shifts). Wavelet analysis can be compared to Fourier analysis because it also splits a signal down into its constituent parts for analysis. Fourier transform breaks the signal into a series of sine waves of different frequencies while the wavelet transform breaks the signal into its "wavelets", scaled and shifted versions of the "mother wavelet".

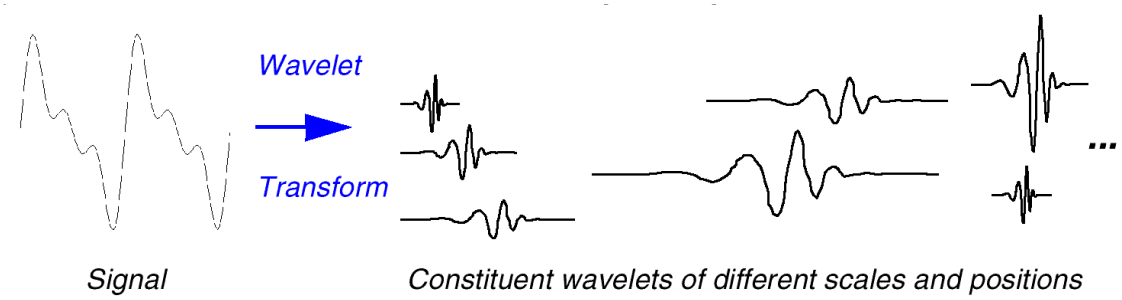

Figure 3.3 Demonstration of Continuous Wavelet Transform

Continuous Wavelet Transform of any signal *y(t)* can be defined as the sum over all time of the signal multiplied by scale , shifted version of the wavelet function *ψ(t)* :

$$CWT(\tau, a) = \frac{1}{\sqrt{|a|}} \int x(t)\psi^*(\frac{t-\tau}{a})dt \qquad 3.4$$

In the Equation 3.4, 'a' and 'τ' represent scale and translation variables, respectively. $\frac{1}{\sqrt{|a|}}\psi(\frac{t-\tau}{a})$ is the scaled and translated mother wavelet, $\psi_{a,\tau}(t)$ and $\frac{1}{\sqrt{|a|}}$ is used for energy normalization across different scales.

$$\psi_{a,\tau}(t) = \frac{1}{\sqrt{|a|}}\psi(\frac{t-\tau}{a}) \qquad 3.5$$

CWT transforms a signal into its time-scale representation. It should be noted that, in wavelet transform, scale is used instead of frequency. By scaling a wavelet, it is either

stretched or compressed. Larger scales result in dilation of wavelet and small scales result in compression of the wavelet. Scale and frequency have an inversely proportional relationship. High frequencies (low scales) correspond to compressed wavelets and give the rapidly changing details of signal while low frequencies (high scales) correspond to expanded (dilated) wavelets and provide the global information of the signal. Figure 3.4 clarifies the concept of scaling.

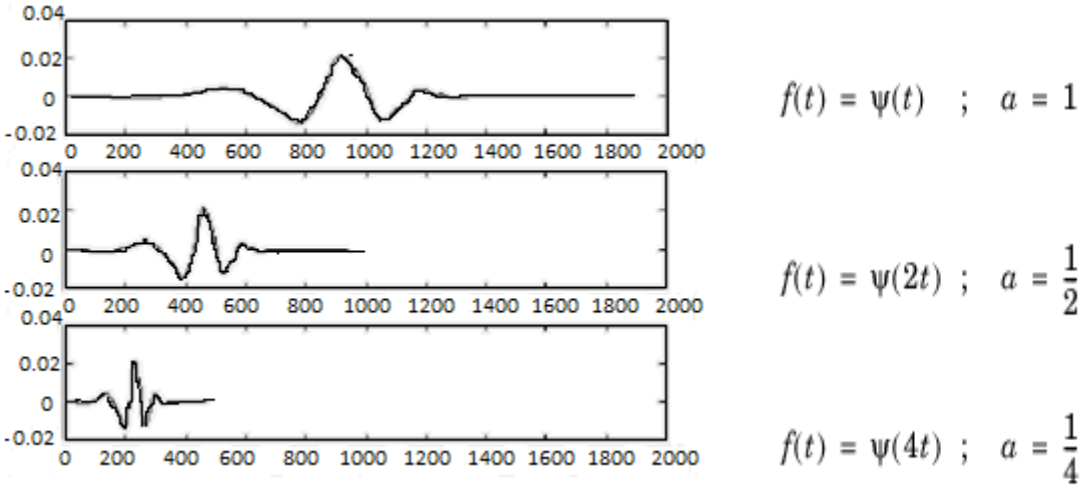

Figure 3.4 Scaling a wavelet

Translation can be compared to the location of window in STFT so it contributes to the time localization in the transform domain. Scale contributes to the frequency localization in the transform domain. Compression and dilation involved in scaling correspond to the ability of wavelet transform to zoom in or zoom out of the signal.

Many different types of wavelets can be used. Type of a wavelet is chosen on the basis of the application. Few commonly used types include Haar, Daubechies, Morlet, Coiflet and Symmet Wavelets. These are shown in Figure 3.5. Haar Wavelet is the simplest and is

best suited for detecting signal discontinuities. Daubechies (db) wavelet family may have different orders. Wavelet functions become more complex with increase in order. db1 refers to Haar Wavelet. Haar wavelet is used in this thesis for detecting discontinuities in TCF phase plot.

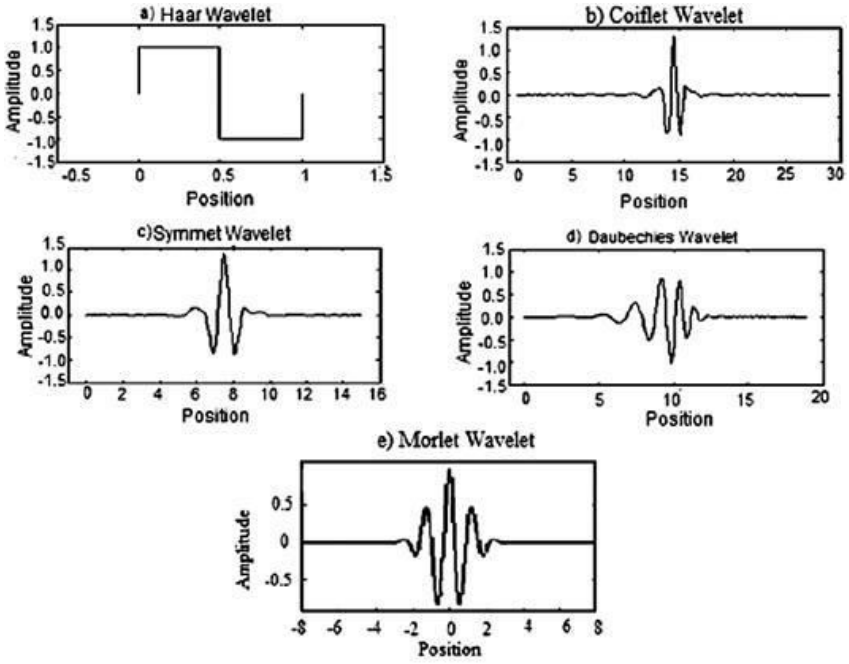

Figure 3.5 Different types of wavelets

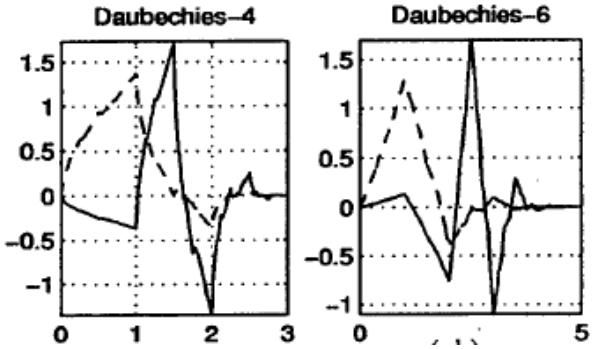

Figure 3.6 db-4 and db-6 wavelets with dashed lines representing scaled functions [7]

3.5 Wavelet Series

As given in Equation 3.4, CWT is computed by shifting a scaled function over a signal and finding the correlation between the two. Both shifting and translation follow

continuous time variation. Resultant wavelet coefficients are therefore highly redundant. This makes CWT redundant and computationally complex as well. Discrete wavelets are used to make the CWT discrete. Discrete wavelets are scaled and translated in discrete steps, instead of the continuous scaling and translation involved in CWT. It requires sampling of the Time-Frequency or Translation-Scale plane. Sampling is done such that the sampling rate is decreased (according to Nyquist's rule) at lower frequencies (higher scales). For instance, if the time-scale plane is sampled with a sampling rate of N_1 at scale s_1, the same plane is sampled with a sampling rate of N_2, at scale s_2, such that, $s_1 < s_2$ (frequency $f_1 > f_2$) and $N_1 > N_2$. It can be stated as

$$N_2 = \frac{s_1}{s_2} \mathrm{N}_1 \qquad 3.6$$

When stated in terms of frequency, it can be said that high sampling rate is used for high frequencies and vice versa. Nyquist sampling rate is the minimum sampling rate required for perfect reconstruction of the original time domain signal. In application where synthesis is not required and only analysis is to be carried out, there is no compulsion of Nyquist rate for discretization.

The Translation-Scale plane is made discrete in such way that the scale parameter **s** is represented by a logarithmic grid. Discretization of time parameter is done with respect to the scale parameter, i.e., a different sampling rate is used for every scale. So, the sampling is carried out on a dyadic sampling grid as shown in Figure 3.7. CWT gives a value to the all the points on this plane. Consequently, number of CWT coefficients is infinite. When the scale axis is observed, it can be noted that out of the infinite number of points, only a finite number are considered by employing a logarithmic law. The base of the logarithm is commonly taken as **2** for ease. When 2 is used, only the scales 2, 4, 8, 16, 32, 64,...etc. are calculated. The time axis is discretized in accordance with the discretization of the scale axis.

As the discrete scale differs by factors of **2**, the sampling rate also decreases for the time axis by a factor of **2** at every scale. Such a discrete grid is referred to as dyadic grid.

Figure 3.7 shows that at the lowest scale (s = 1), 24 samples are taken along the time axis. At the next scale value, s = 2, the sampling rate of time axis reduces by a factor of 2 for increase in scale by a factor of 2, and hence, 12 samples are taken. At the next step, s = 4, only 6 samples are taken in time, and so on.

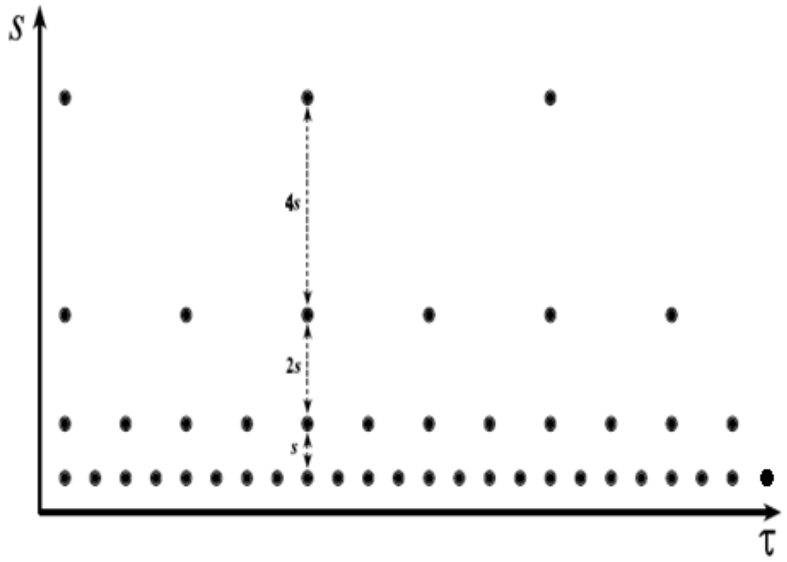

Figure 3.7 Translation-Scale Dyadic Grid [10]

For Discrete Wavelets, equation 3.5 can now be modified as:

$$\psi_{j,k}(t) = \frac{1}{\sqrt{s_0^j}}\,\psi\left(\frac{t - k\tau_0 s_0^j}{s_0^j}\right) \qquad 3.7$$

In equation 3.6, 'j' and 'k' represent integers; $s_0 > 1$ refers to dilation (scale discretization) and τ_0 is the translation discretization factor which is determined by s_0. s_0 is usually chosen as 2 and the translation factor is chosen as $\tau_0 = 1$, so that the sampling

of both frequency and time axis is called *dyadic sampling*. So equation 3.6 can now be modified as:

$$\psi_{j,k}(t) = \frac{1}{\sqrt{2^j}}\,\psi\left(\frac{t-k2^j}{2^j}\right) \qquad 3.7$$

A series of wavelet coefficients is obtained when discrete wavelets are used to transform a continuous signal. This is called *wavelet series decomposition*.

3.6 Discrete Wavelet Transform

Wavelet series, discussed in the previous section, is just a sampled form of the CWT, not a discrete transform. The information provided by wavelet series is highly surplus if the reconstruction of the signal is specifically focused upon. Discrete Wavelet Transform (DWT) reduces the computation time and also gives enough information for both analysis and reconstruction of the signal. DWT is comparatively easy to implement as opposed to CWT.

In Discrete Wavelet Transform, digital filtering methods are utilized to get a time-scale representation of a digital signal. Continuous Wavelet Transform gives a correlation between a signal and wavelet at different scales and translations. CWT is calculated by altering the scale of the analysis window (wavelet), changing its time shift, multiplying by the signal, and integrating with respect to time. In DWT, filters of different cutoff frequencies are used to examine the signal at different frequencies (scales). The signal is passed through a number of high pass filters and low pass filters to study the high frequency and low frequency components of the signal, respectively.

The filtering operations change the resolution of the signal and the scale is changed by upsampling and downsampling operations.

The concepts involved in DWT are explained in greater detail as follows.

3.6.1 Band-pass filter

An important property of wavelets is admissibility condition. It means that the Fourier Transform of the wavelet function is zero at dc, that is

$$|\psi(\omega)|^2|_{\omega=0} = 0 \qquad 3.8$$

This implies that wavelet should have a band-pass type spectrum. Fourier analysis tells that compression of a signal in time-domain stretches its spectrum in frequency-domain. Mathematically it can be stated as:

$$F\{f(at)\} = \frac{1}{|a|} F\left(\frac{\omega}{a}\right) \qquad 3.9$$

Equation 3.8 shows that compression of the wavelet in time by a factor of 2 will stretch the frequency spectrum of the wavelet by a factor of 2 and will also move all frequency constituents up by a factor of 2. This approach can be used to cover the frequency spectrum of the signal with the spectrums of dilated wavelets in the same way as that the signal is covered in the time-domain with translated wavelets. So a series of dilated wavelets can be considered as a band-pass filter bank. The ratio between the center frequency of a wavelet spectrum and the width of this spectrum is the same for all wavelets. This ratio is called the fidelity factor Q of a filter. Wavelets are characterized as *constant-Q* filters.

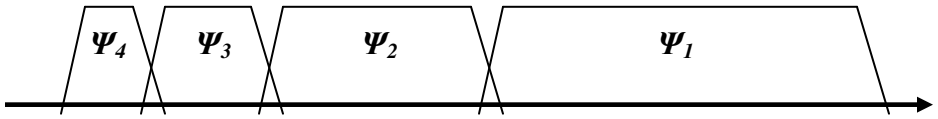

Figure 3.8 Wavelet Spectrum of the mother wavelet that is scaled in time [10]

3.6.2 Scaling Function

In Multi-Resolution Analysis (MRA), a scaling function provides a series of approximations of a signal, such that each differs by a factor of 2 in scale (or resolution) from its neighboring approximations. Wavelets provide the difference in information between adjacent approximations. Scaling functions together with wavelets are used to analyze the signal. The scaling function actually solves the issue of the infinite number of wavelets required to cover the spectrum down to zero and lays down a lower limit for wavelets. A wavelet has a band-pass spectrum and a scaling function has a low-pass spectrum, so a series of dilated wavelets along with a scaling function can be considered as a filter bank. Figure 3.9 clearly depicts this concept.

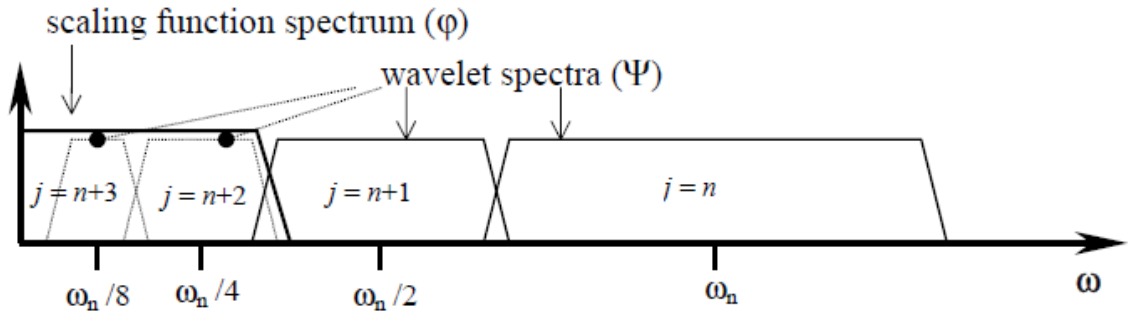

Figure 3.9 Concept of Scaling Function

Scaling function may be mathematically defined as:

$$\varphi_{j,k}(t) = \frac{1}{\sqrt{2^j}}\,\varphi\left(\frac{t-k2^j}{2^j}\right) \qquad 3.10$$

$$\varphi_{j,k}(t) = 2^{j/2}\varphi(2^j t - k) \qquad 3.11$$

Here j, k are integers and $\varphi(t)$ ϵ $L^2(R)$. $L^2(R)$ denotes the set of measurable, square-integerable functions; R is set of real numbers. K determines the position of $\varphi_{j,k}(t)$ and j

determines the width of$\varphi_{j,k}(t)$. The term $2^{j/2}$ controls the amplitude of function. Since the shape of $\varphi_{j,k}(t)$ changes with 'j', it is called a scaling function.

$\{\varphi_{j,k}(t)\}$ is a set of expansion functions made up of binary scaling and integer time shifts of $\varphi(t)$. It spans a subspace of $L^2(R)$. Subspace spanned over 'k' for any 'j' can be defined as [11]:

$$V_j = \overline{\text{Span}_k \{\varphi_{j,k}(t)\}} \quad 3.12$$

With the increase in 'j', the size of V_j increases and $\varphi_{j,k}(t)$ which is used to represent the subspace functions becomes compressed.. This allows functions with fine details to be included in the subspace. At low scales, the subspaces covered by the scaling function are enclosed within subspaces spanned at higher scales. If a function, g(t) is an element of V_0, it is also an element of V_1. It means all V_0 expansion functions lie within V_1. Mathematically it can be stated as $V_0 \subset V_1$. The reference subspace V_0 is arbitrarily chosen. A general representation is:

$$V_{-\infty} \subset \ldots \subset V_{-1} \subset V_0 \subset V_1 \subset V_2 \subset \ldots \subset V_{\infty} \quad 3.13$$

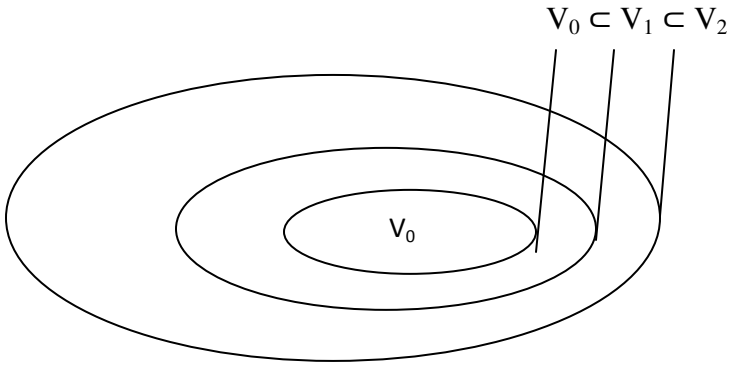

Figure 3.10 Function subspaces spanned by a scaling function [11]

3.6.3 Wavelet Functions

A wavelet function $\psi(t)$ along with its binary scaling and integers translates, provides the difference between any two adjacent subspaces V_j and V_{j+1}.

If W_j is the space spanned by $\psi_{j,k}(t)$, it can be stated as [11]:

$$W_j = \overline{\text{Span}_k \{\psi_{j,k}(t)\}} \quad 3.14$$

Now the wavelet and scaling function subspaces can be linked together as:

$$V_{j+1} = V_j \oplus W_j \quad 3.15$$

In equation 3.15, $\oplus$ represents the union of spaces. V_j and W_j represent the scaling function and wavelet function subspaces.

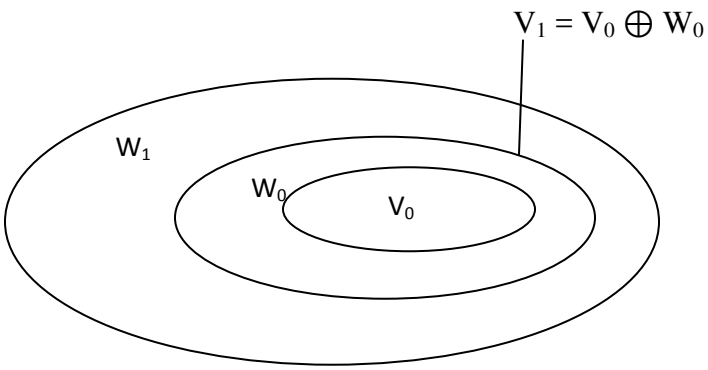

Figure 3.11 Relationship between wavelet and scaling functions [11]

The expansion functions of a scaling function subspace V_j is represented as weighted sum of the expansion functions of the next higher resolution subspace V_{j+1}.

$$\varphi_{j,k}(t) = \sum_n h_\varphi(n) 2^{(j+1)/2} \varphi(2^{(j+1)} t - n) \quad 3.12$$

Equation 3.12 is called the dilation equation [11]. $h_\varphi(n)$ are called the scaling function coefficients. They refer to the sub-band coding low pass filter coefficients. Similarly,

expansion functions of the wavelet function subspace W_j can also be written as weighted sum of the expansion functions of next higher resolution subspace W_{j+1}.

$$\psi_{j,k}(t) = \sum_n h_\psi(n) 2^{(j+1)/2} \psi(2^{(j+1)} t - n) \quad 3.13$$

Here $h_\psi(n)$ are called the wavelet function coefficients. They refer to the sub-band coding high pass filter coefficients.

3.6.4 Sub-band Coding

Sub-band coding refers to the decomposition of the signal into a set of band-limited components (sub-bands). The decomposition is carried out by means of digital filter banks. Digital filters of different cutoff frequencies are used to examine the signal at different frequencies (scales). The signal is passed through a number of high pass filters and low pass filters to study the high frequency and low frequency constituents of the signal, respectively.

Sub-band coding algorithm starts with passing the signal through a half band low pass filter (having an impulse response of h[n]) and a half band high pass filter (having an impulse response of g[n]). Low pass filter removes all frequencies that are above half of the highest frequency in the signal. Similarly high pass filter removes all frequencies below half of the highest frequency in the signal. This methodology splits the frequency components of the signal into two sub-bands. If the original signal has the highest frequency component of 'q' radians then according to Nyquist's rule its sampling frequency would be '2q' radians. After half band filtering, the highest frequency component of the filter's output will be halved to 'q/2' radians. So according to Nyquist's rule, its sampling frequency should be 'q' radians. It means half the samples are

redundant. Sub sampling by 2, thus removes half of the samples. Filtering is followed by subsampling by 2. The decomposition procedure is repeated by successive filtering and downsampling. At each level filtering and downsampling will give half the number of samples (half the time resolution) and half the frequency band spanned (double the frequency resolution). Figure 3.12 demonstrates the sub-band coding methodology, where x[n] is the original signal. Low pass filer is represented by h[n] and high pass filter is represented by g[n]. Each filter's bandwidth is marked as 'f'.

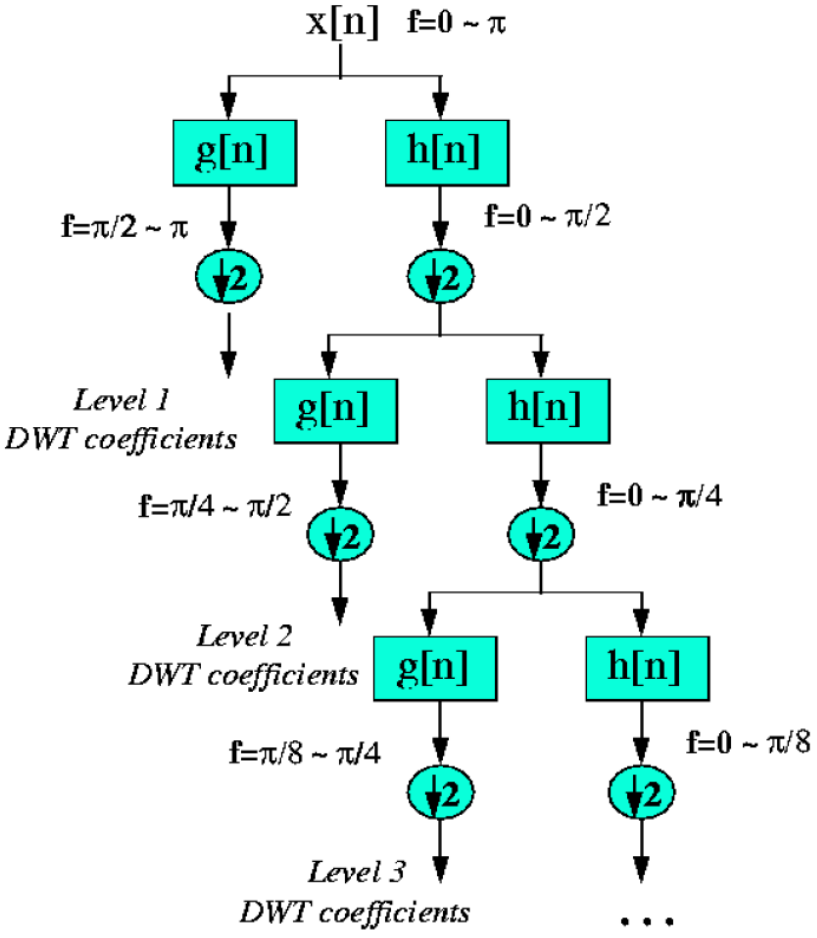

Figure 3.12 Sub-band Coding Demonstration

Figure 3.12 shows that each high pass filter's output (after subsapmling) gives the DWT coefficients for the corresponding level of decomposition. The process of filtering and downsampling can be mathematically depicted as:

$$y_{hp}[n] = \sum_k x[k].g[2n-k] \quad 3.14$$

$$y_{lp}[n] = \sum_k x[k].h[2n-k] \quad 3.15$$

In the above equations $y_{hp}[n]$ and $y_{lp}[n]$ correspond to the high pass and low pass filter outputs (after downsampling by 2), respectively. For perfect reconstruction, the impulse responses of high pass and low pass filters should be related as:

$$g[K - 1 - n] = (-1)^n . h[n] \quad 3.16$$

In equation 3.16, g[n] and h[n] are the high pass and low pass filter impulse responses, respectively. 'K' is the length of the filter (in terms of filter coefficients). Filters that satisfy the condition in equation 3.16 are called Quadrature Mirror Filters.

Any function, x(t) can be expanded as:

$$x(t) = x_a(t) + x_d(t) \quad 3.17$$

where, $x_a(t)$ is an approximation of the function x(t), using V_0 scaling functions, and $x_d(t)$ is the difference between the function x(t) and its approximation expressed as a sum of W_0 wavelets. The low frequencies of x(t) are given by $x_a(t)$ (it gives the average value of x(t) in every integer interval). On the other hand, $x_d(t)$ gives the detail. When described in terms of the iterative filter bank, the low pass filter provides the approximation and the high pass filter gives the detail coefficients.

3.7 Benefits of Wavelet Analysis

The advantages of Wavelet Analysis can be summarized as below:

1. Wavelets provide a simultaneous localization both in time and frequency domain.

2. Fast wavelet transform makes it very fast computationally.
3. Wavelets are able to distinguish the minute details in a signal. Very small wavelets are best suited to isolate very fine details in a signal, while very large wavelets identify coarse details.
4. Data compression and perfect reconstruction can be obtained by using Wavelet Theory.
5. Wavelet Analysis provides a good approximation of a given function or signal by using only a few coefficients which is the great accomplishment as compared to Fourier transform.
6. Wavelet transformation is capable of showing those aspects of data that other signal analysis techniques miss, such as breakdown points, and discontinuities in higher derivatives and self-similarity.
7. It has the ability to remove noise from a signal or image without considerable deprivation of the signal's characteristics.
8. Wavelet Transform along with its many variants is widely used in Image Processing for edge detection.

3.8 Detecting Discontinuities and Breakdown Points using Wavelets

Frequency hopping spread spectrum signals undergo abrupt changes in frequency. Fourier analysis is usually not able to detect these jumps. Wavelets are best suited for finding out abrupt transitions in a signal or any of its high order derivatives. For this purpose, the chosen wavelet should be able to represent the highest order derivative present in the signal function. Any wavelet with, at least, p vanishing moments can be

used to detect a discontinuity in the p - 1 derivative [7]. Figure 3.13 shows few types of mother wavelets that can be used for detecting discontinuities.

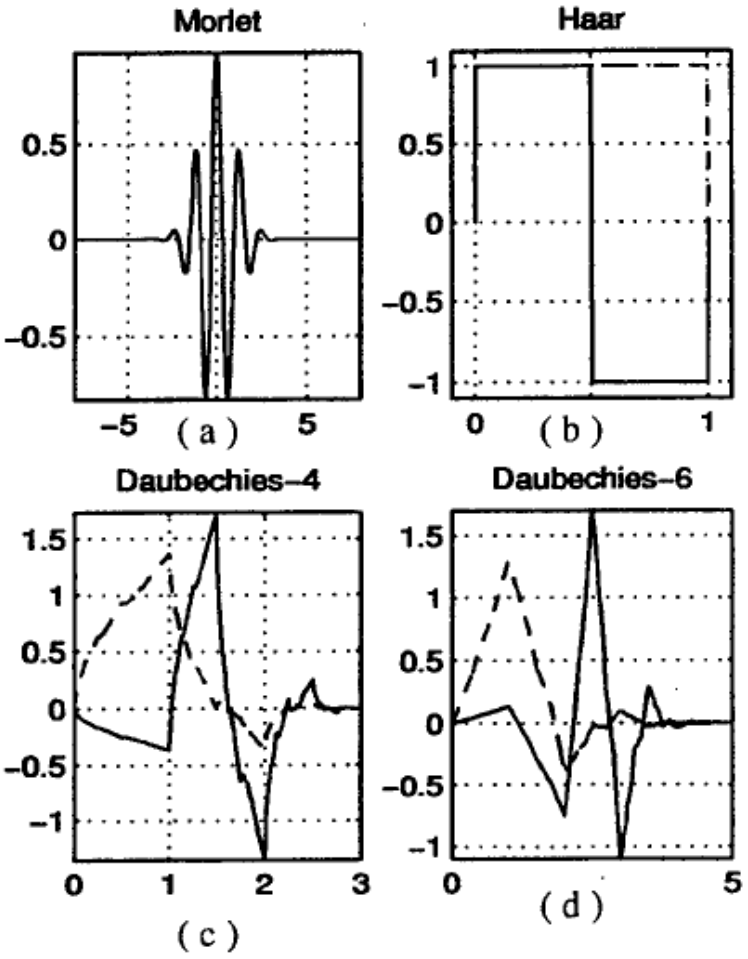

Figure 3.13 Wavelets with their scaling functions shown with dashed lines [7]

Haar wavelet is the shortest of all wavelets and is, therefore, best suited for detecting discontinuities in a signal. It has only one vanishing moment and hence can only detect discontinuity in the p – 1 = 0 derivative (i.e. the signal itself). db-4 and db-6 have 2 and 3 vanishing moments, respectively. They are hence, able to detect discontinuity in the first and second derivative of the signal, respectively.

Concepts developed in this chapter are utilized in the Detection and Hop Time Estimation Algorithm discussed in the following chapter. The phase discontinuity in the processed TCF plot can be considered a high frequency signal and after applying Discrete Wavelet Transform (DWT) along with further signal processing, detection and hop time evaluation of the sample FH signal is carried out. The next chapter explains all the steps of the algorithm in complete detail.

Chapter 4

DETECTION AND HOP TIME EVALUATION ALGORITHM

Based on the concepts described in chapter 2 and 3, Detection and Hop Time Evaluation Algorithm for a Frequency Hopping Spread Spectrum (FHSS) signal can now be explained stepwise.

4.1 Algorithm Steps

1. First step involves signal generation. General form of a frequency hopping signal can be written as [12]:

$$x(t) = A\sum_k rect_{T_h}(t - kT_h - \theta)e^{j2\pi f_k(t-kT_h-\theta)} + w(t) \qquad 4.1$$

Here $0 < t < T$, $w(t)$ is Additive white Gaussian Noise, f_k is a hop frequency in the spread bandwidth.

$$rect\ T_h\ (t) = \begin{cases} 1 & t \in (-\frac{T_h}{2}, \frac{T_h}{2}) \\ 0 & elsewhere \end{cases}$$

In this work, a two-hop Frequency Hopping system model is considered for applying the algorithm. So the analytic form of the two-hop frequency hopping signal would be as follows [12]:

$$x_a(k) = e^{j2\pi f_1 k}\left[u(k) - u\left(k - T_{hop}\right)\right] + e^{j2\pi f_2 k}\left[u\left(k - T_{hop} + 1\right) - u(k - T)\right] \qquad 4.2$$

for $0 \leq k \leq T$,

T_{hop} is the time of hop of the signal from one frequency f_1 to f_2 and u(k) is the unit step function.

2. An assumption is made about the minimum hop time, T_{hop_min}. Value of T_{hop_min} is taken as 256 samples. Based on this assumption, data is segmented into frames of length equal to 256. This assures that there is at most one hop in a frame.

3. Temporal Correlation Function (TCF) is computed for each frame. The phase of TCF is plotted, as described in Chapter 2.

4. The TCF phase is unwrapped along the time axis for a fixed value of lag, τ. Phase unwrapping eliminates the discontinuities, in the cross-term region of TCF phase plot, due to periodicity in phase and also reduces the spikes due to noise.

5. A median filter of length 5 is applied to the unwrapped TCF phase. This step reduces the effect of noise.

6. The unwrapped, median filtered, TCF phase is differentiated with respect to time. This changes the ramp in the TCF_{12} phase region into a pseudo pulse.

7. A second median filter of length 25 is applied to the processed TCF phase, along time axis. This is also a de-noising technique.

8. Discrete Wavelet Transform (DWT) is computed using Haar Wavelet. This is used to identify the discontinuities at the boundaries of the cross-terms region of the TCF phase obtained in the previous step.

9. Haar Wavelet exactly detects discontinuities in no-noise case but its ability of detection is adversely effected with the occurrence of noise. To counteract this issue, averaging of scales is done. So the DWT detail coefficients of the first two scales, d1 and d2 are summed up. In MATLAB, DWT transformation automatically downsamples the filter's output by two. In order to keep the same dimension as that of the original TCF phase plot, upsampling by 2 is done by taking $d2(2n+1) = d2(2n)$, for $n = 0,1,2,\ldots,N-1$.

N is the length of d2. Upsampling is done before summation.

10. Detection vector is obtained by doing 45˚/135˚ summation across all values of lag, τ. The detection vector is represented with respect to time.

11. The resulting detection vector is compared with a threshold. This detects the presence of hop in the signal.

12. The detection vector shows a peak at the time of frequency hop. The time index corresponding to the peak in the detection vector gives the estimated hop time of the Frequency Hopping Spread Spectrum signal.

This chapter, now, describes the simulation process and further clarifies the algorithm by applying it to a sample frame.

4.2 System Model

MATLAB simulations are carried out to test the Detection & Hop Time Estimation Algorithm explained in the previous section.

The Frequency Hopping Signal is generated with the following specifications:

a) Frequency Bandwidth used for spreading: 2 – 30 MHz (HF Band)

b) Sampling Frequency, f_s = 60 MHz

c) Signal is segmented into frames, with each frame having a length of $T_{hop\text{-}min}$

d) $T_{hop\text{-}min}$ is taken as 256 sample points. This assumption is made so as to make sure that there will be one hop in each frame, at maximum. With the sampling frequency of 60 MHz, the minimum hop time comes out to be 4.27μs.

e) Minimum frequency differential Δf = 2kHz

f) No. of hop frequencies in the spread bandwidth, $N_f = (f_{max} - f_{min})/ \Delta f$

N_f = (30 – 2) MHz/ 2kHz = 14,000

g) With the above mentioned specifications, the frequency hopping signal thus generated either has

i) no hop in a frame, or

ii) it has a hop from any frequency f_1, to any frequency f_2, such that

2 MHz $\leq f_1, f_2 \geq$ 30 MHz, and $|f_1 - f_2| \geq$ 2kHz

The Frequency Hopping Signal is generated by taking a random hopping time, T_{hop}, in the 256 point sample frame (between sample point 26 and 231). The twenty five samples at the start and end of a frame are not considered due to problems caused by edge effects. If a hop occurs within a simulation frame (i.e. when $T_{hop} \neq 0$), then both frequencies before and after the hop are randomly generated. This results in a signal with, not more than, one frequency hop from f_1 to f_2, in the spread bandwidth such that

2 MHz $\leq f_1, f_2 \geq$ 30 MHz, and $|f_1 - f_2| \geq$ 2kHz

Simulation involves five hundred experiments, that are carried out with six different SNR values, varying from 15dB to -3dB. The algorithm determines

a) Presence of a frequency hop in the frame

b) The hop time estimate, in case of a frequency hop within a frame

Out of the 500 trial experiments, 10% of the randomly generated hop times are taken as zero to completely test the effectiveness of the algorithm.

In the simulations, SNR is defined as:

$$SNR = 10log_{10}(\frac{p_{signal}}{\sigma^2_{noise}}) \quad 4.3$$

Here p_{signal} is the signal power and σ^2_{noise} is the noise variance. For a signal with unity amplitude, equation 4.3 becomes

$$SNR = 10log_{10}(\frac{1/2}{\sigma^2_{noise}}) \quad 4.4$$

From equation 4.3, the Standard Deviation of Additive White Gaussian Noise can be computed as:

$$\sigma_{noise} = \sqrt{\frac{1}{2}\ 10^{-SNR/10}} \quad 4.5$$

4.3 Detection and Parameter Estimation Algorithm Applied to a Sample Frame

In order to develop a complete understanding of the detection and hop time estimation of the FHSS signal carried out in this work, it is applied to a sample frame.

4.3.1 Signal Generation

A simulation frame of length 256 samples has a randomly generated hop time, T_h of 139. The frequencies before and after the hop are 25.89 MHz and 24.2MHz, respectively. i.e. $\mathbf{f_1}$=25.89 MHz, $\mathbf{f_2}$=24.2 MHz and $\mathbf{T_h}$= 139 samples. After adding AWGN, the resulting SNR is 10 dB.

4.3.2 Temporal Correlation Function (TCF)

The phase of the TCF expression given in equation 2.8 is plotted for the simulation frame under consideration in figure 4.1. In the figure, TCF phase is plotted, with time, t along the y-axis and lag, τ along the x-axis .The bottom triangle (TCF_1 (t,τ) region) is obtained by the auto-terms at frequency, f_1 and the top triangle (TCF_2 (t, τ) region) is obtained by the auto-term at frequency, f_2. The cross-terms region TCF_{12} (t, τ) is due to both $f_1$and f_2. Moreover, the cross-terms region is centered on the hop time, i.e. t = T_{hop}, for $0 \leq \tau \leq T_{hop}$.

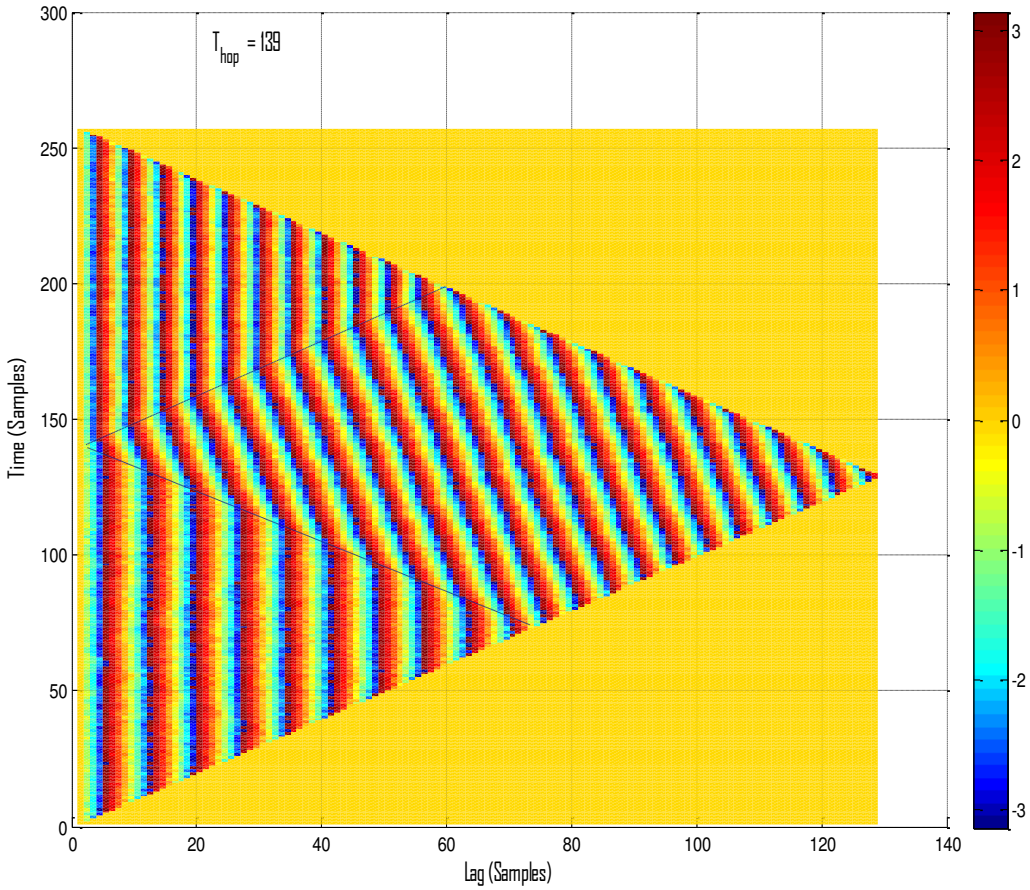

Figure 4.1 TCF Phase plot with $\mathbf{f_1}$=25.89 MHz, $\mathbf{f_2}$=24.2 MHz and $\mathbf{T_h}$= 139 samples

When observed for a fixed value of lag, the phase is constant with time in the TCF_1 (t, τ) region, shows phase variations in the TCF_{12} (t, τ) cross-terms region and then the phase again becomes constant in the TCF_2 (t, τ) region. Figure 4.2 shows the TCF phase for a fixed lag of τ = 25. The presence of noise causes random spikes in the phase information. Detection and hop time estimation process is determined by the changes in the TCF phase behavior in the three regions.

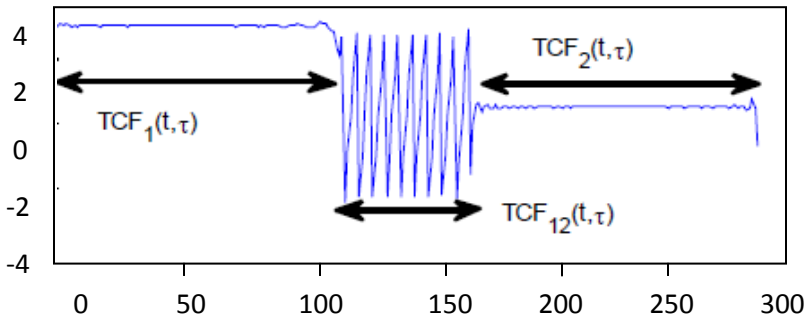

Figure 4.2 TCF phase for lag, τ = 25 with no-noise [6]

Figure 4.3 shows the TCF phase for lag, τ = 25 distorted by AWGN. It is clear from the Figure that for a FH signal distorted by noise, the detection and hop time estimation becomes difficult. TCF_1 (t, τ) and TCF_2 (t, τ) regions also show phase variations instead of constant phase.

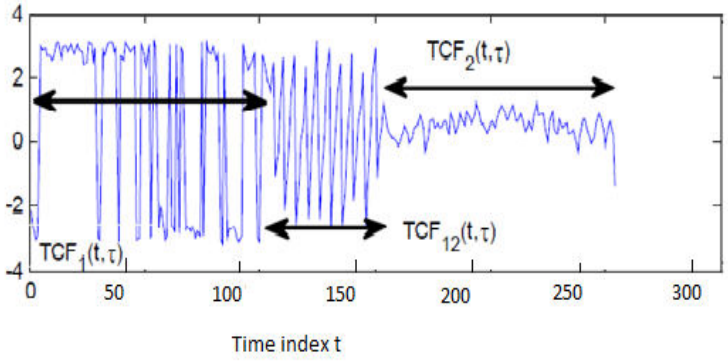

Figure 4.3 TCF phase for lag, τ = 25 with SNR = 10dB [6]

4.3.3 Pre-processing Techniques

Steps 4 – 7 of the algorithm described in section 4.1, are the pre-processing methods used to de-noise the TCF phase of the analytic FH signal. Phase behavior is normally very sensitive to noise degradation. It is for this reason that few pre-processing steps are added to minimize noise effects. These techniques include phase unwrapping, median filtering and differentiation.

Unwrapping the TCF phase for a fixed value of lag, τ removes the phase discontinuities due to periodicity of 2π in phase. It makes the phase linear in the TCF_{12} region resulting in a ramp. The TCF_1 and TCF_2 regions show constant phase at different levels.

Median filtering de-noises the TCF phase information while preserving the discontinuities between the regions. A median filter of length 5 is applied before differentiation and a second median filter of length 25 is again applied after differentiation.

Differentiation changes the ramp into a pseudo-pulse and the constant phase regions become zero after differentiation. This step results in a pseudo-pulse whose height is equal to the slope of the unwrapped TCF phase and its width is equal to the width of cross-terms region, and centered on $\boldsymbol{T_{hop}}$ (i.e. centered at sample point 139 of the time axis for the simulation frame under consideration)

All the pre-processing techniques have been discussed in detail in section 2.4.

4.3.4 Detecting Discontinuities using DWT

Steps 8 and 9 of the algorithm are applied to the pseudo-pulse obtained after differentiation and median filtering of the unwrapped phase of TCF. Discrete Wavelet Transform is computed using Haar Wavelet. DWT detects discontinuities at the rising

and falling edges of the pulse. After this, the wavelet coefficients of the first two scales are added to minimize the effect of noise. This technique is called averaging of scales. The concept behind is that when two or more scales are summed up and clipped at some threshold, the true discontinuities line up across all scales while the spikes due to noise do not line up. Figure 4.4 clarifies the concept where Discrete Wavelet Transform of a noisy stair step function is computed for six scales using Haar Wavelet. The coefficients of six scales are added and compared against a threshold. Thus by using averaging of scales, all the step times can be computed even in the presence of noise.

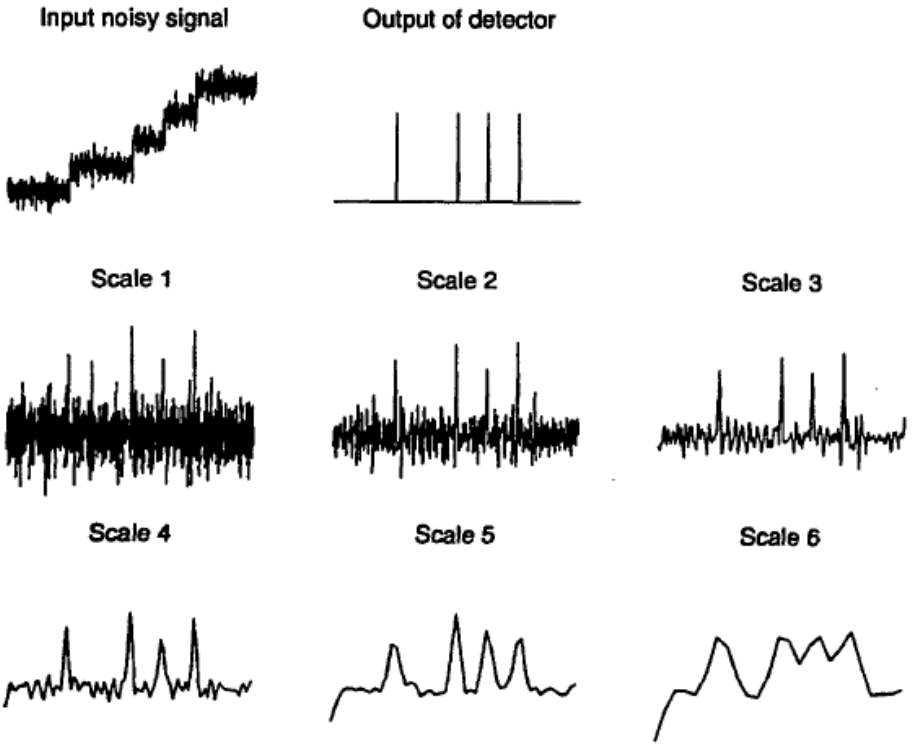

Figure 4.4 Detection of stair step times using averaging of scales [7]

DWT transformation in MATLAB inherently downsamples the filter's output by two. To keep the same dimension as that of the original TCF phase plot, upsampling by 2 is done by taking d2(2n+1) = d2(2n), for n = 0,1,2,…,M-1.

M is the length of d2. Upsampling is done before summation.

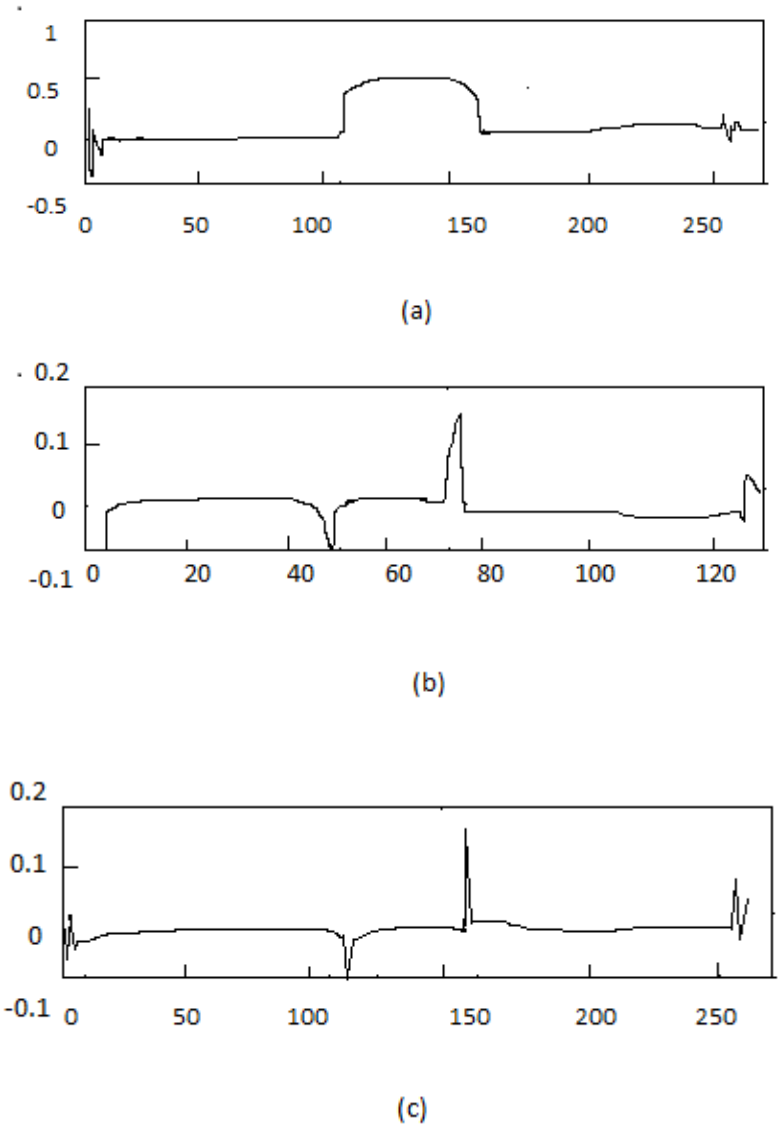

Figure 4.5 DWT of the processed TCF phase for a constant $\tau = 25$, (a) After median filtering (of length 25) of the differentiated unwrapped TCF phase, (b) Level 1 detail coefficient of DWT, Haar wavelet, (c) Level 1 detail coefficient of DWT upsampled by 2

4.3.5 Detection Vector

In step 10 of the algorithm, detection vector is computed. It is obtained by doing 45˚/135˚ summation on the Discrete Wavelet Transform matrix. All values representing the edges

of the cross-terms region in the processed TCF phase are summed up. The result of summation emphasize at the hop time, T_{hop}. Detection vector is represented with respected to time. It gives peak amplitude at the hop time.

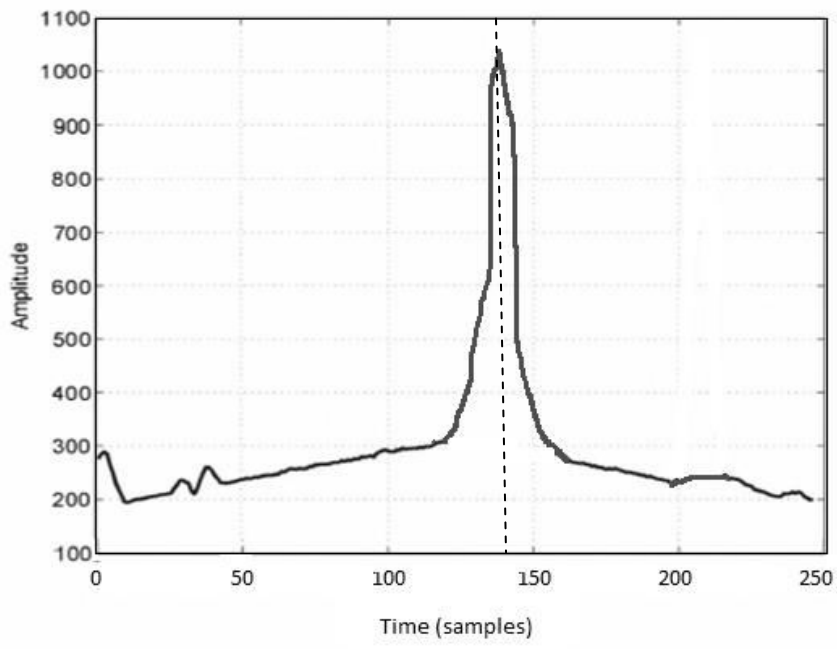

Figure 4.6 Detection Vector

4.3.6 Determination of Threshold

After getting the detection vector, decision is required to be made about the presence of hop in the simulation frame. It has been experimentally shown that variance of the detection vector is the figure that can be best utilized to detect the presence of a frequency hop. Variance is actually a measure of the spread between amplitudes in a data set. Therefore, the variance of the detection vector having no hop is considered a reference for threshold calculation. $T_{threshold}$ is taken as a constant times the variance of the detection vector with no hop for a given value of SNR.

$$T_{threshold} = k.\ \text{variance}\ (\text{detection vector}_{\text{no hop}}(t)) \quad 4.6$$

Determination of threshold is directly related to the probability of missed detections. Probability of detection, P_D and probability of missed detection, P_m are related as follows:

$$P_m = 1 - P_D \qquad 4.7$$

The value of the multiple, k, in equation 4.6, is chosen so as to have a good probability of detection along with a reasonable probability of false alarm.

Probability of missed detections is far more important to focus upon than probability of false alarm, P_{FA}. Hop time estimation is the first stage of the Frequency Hopping signal Demodulation so frequency analysis in the case of a false alarm will result in the same frequency values in two or more successive hop durations. This will not cause any information loss. On the contrary, when any detection is missed, the frequency analysis will result in errors in the demodulated message.

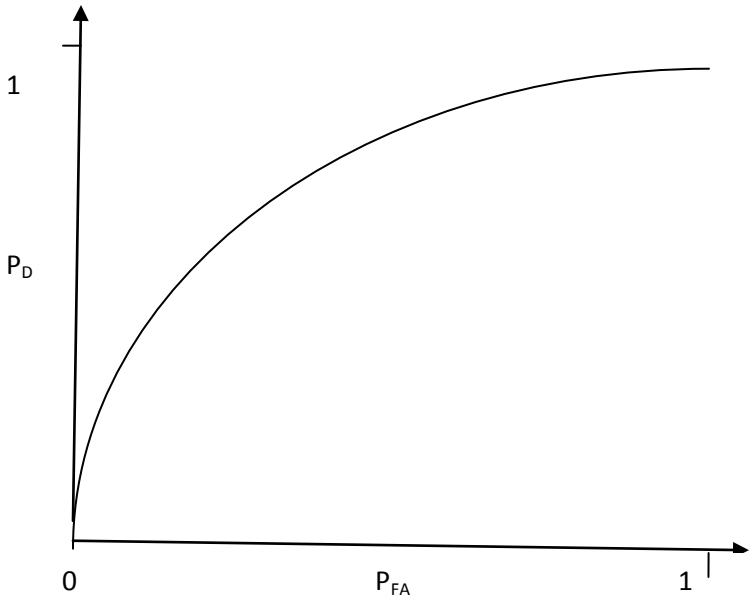

Figure 4.7 A typical Receiver Operating Characteristic Curve

Receiver Operating Characteristics (ROC) curves are used to illustrate the detection performance. ROC curve is a graphical representation of probability of detection, P_D (y-

axis) versus the probability of false alarm, P_{FA} (x-axis). Figure 4.7 shows how an ROC curve generally looks like. SNR of the signal is depicted by the "bow" in the curve. The more the SNR, the more the curve will bend upwards. ROC is plotted by varying the threshold and plotting the corresponding values of P_D and P_{FA}.

4.3.7 Detection of hop

For each of the six SNRs, the ROC curve along with the Probability of Detection (P_D) versus Threshold multiple (k) and the Probability of False Alarm (P_{FA}) versus Threshold multiple (k) plots, are used to determine the threshold. Figure 4.8 illustrates the procedure. Plots correspond to an SNR of 10 dB. To get a P_D of 0.987, the corresponding P_{FA} from ROC curve is 0.05. Now for these values of P_D and P_{FA}, the value of the Threshold multiple, k is chosen from "P_D versus k" and "P_{FA} versus k" plots, as shown in Figure 4.8. The value of k is 30, so from Equation 4.6, the value of Threshold, $T_{Threshold}$ will be 30 times the variance of detection vector obtained with no hop in the frame. The variance of the detection vector constructed for each frame is compared against this Threshold. When the detection vector variance exceeds this threshold, a hop is detected and if the detection vector variance is less than the threshold, no hop is detected.

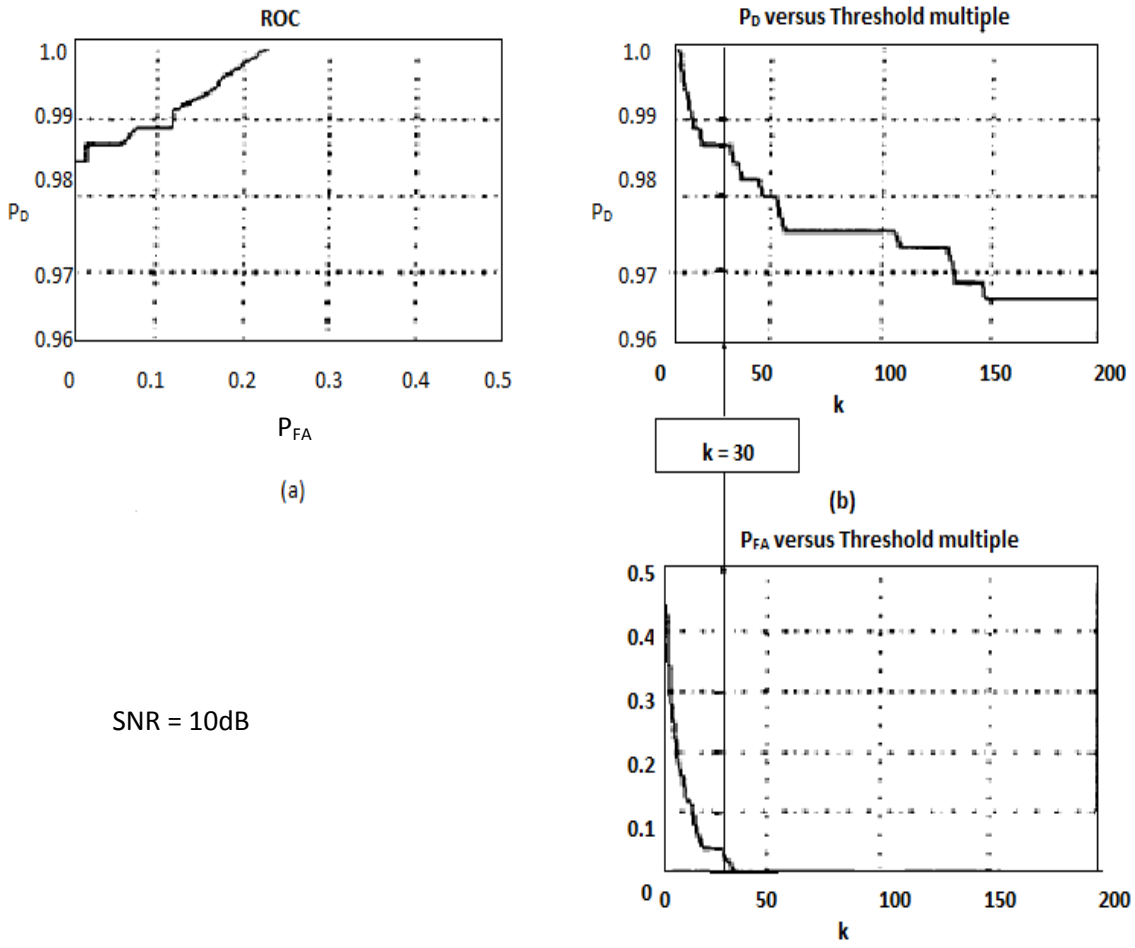

Figure 4.8 Threshold Determination, (a) ROC curve, (b) P_D vs Threshold multiple and P_{FA} vs Threshold multiple

4.3.8 Hop Time Estimation

The time corresponding to the peak amplitude of the detection vector as shown in Figure 4.6, provides the estimated hop time. The difference between the actual hop time and the estimated hop time gives the percentage of error.

The following chapter gives the results of simulations in the form of detection statistics and plots.

Chapter 5

SIMULATION RESULTS

The results of simulations obtained by applying the Detection and Hop time Estimation Algorithm are described below:

5.1 Detection

Table 5.1, shown below provides the results of detection. Out of the 500 experiments, corresponding to each SNR, 10% of the experiments do not have a hop. It means total hops are 450. Table 5.1 provides the number of detections, number of misses, number of false alarms and also the number of "no detections" in case of no hop in the frame.

SNR (dB)	Total hops	detections	misses	False alarms	No hop no detection
15	450	449	1	2	48
10	450	446	4	15	35
6	450	445	5	20	30
3	450	432	18	25	25
0	450	420	30	20	30
-3	450	236	214	13	37

Table 5.1 Detection Results

The performance of a detection algorithm is determined by the probability of detection and the probability of false alarm. A high probability of detection (i.e. a low probability of missed detection) is required along with an acceptable probability of false alarm. For each SNR, the probability of detection and probability of false alarm are computed by the following equations:

$$P_D = \frac{no\ of\ detections}{total\ hops} \quad 5.1$$

$$P_{FA} = \frac{no.of\ false\ alarms}{(no.of\ experiments - total\ hops)} \quad 5.2$$

Table 5.2 gives the detection results in terms of probabilities. It gives the probability of detection, P_D, probability of false alarm, P_{FA} and the percentage of error corresponding to each of the six values of SNR varying from -3 dB to 15 dB. Percentage of error is determined from the false alarms and misses. It is calculated as follows:

$$\%age\ error = \frac{(false\ alarms + miss)}{no.of\ experiments} \quad 5.3$$

SNR (dB)	**k**	**P_D**	**P_{FA}**	**%age error**
15	140	0.998	0.04	0.6
10	30	0.991	0.3	0.8
6	15	0.989	0.4	5.0
3	11	0.960	0.5	8.6
0	1	0.933	0.4	10.0
-3	3	0.524	0.26	45.4

Table 5.2 Detection Statistics of 500 simulations corresponding to each SNR

Detection results given in Table 5.2 show that for an SNR of 3 dB, if 8.6% misclassification and a probability of false alarm of 0.5 is acceptable then, 96% of the hops in a frequency hopping signal can be detected. Figure 5.1 shows a plot of Detection Probability P_D versus SNR.

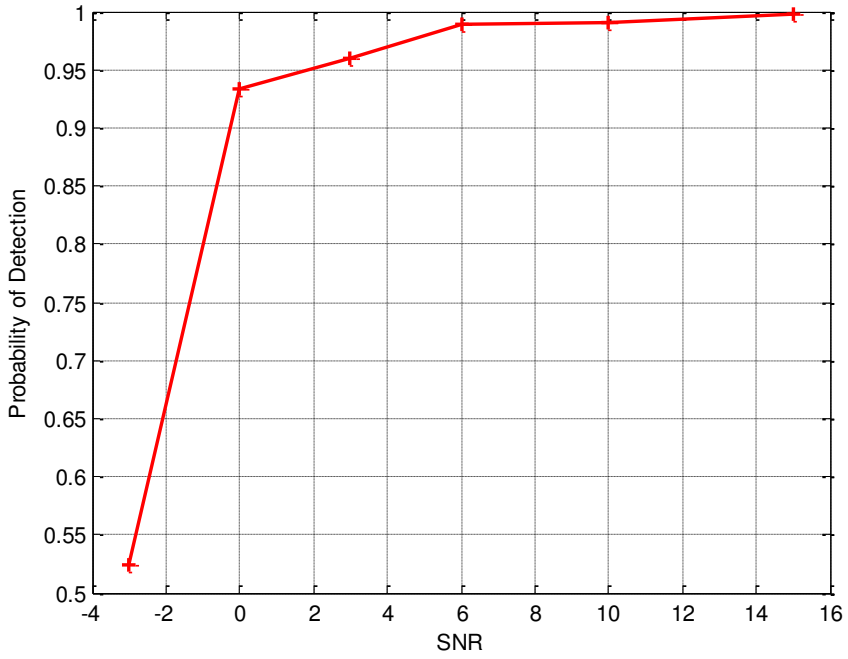

Figure 5.1 Detection Performance

5.2 Hop Time Estimation

The results of hop time estimation are expressed as percentage of the difference from the actual hop time of the frequency hopping signal considered before applying the Detection and Parameter Estimation Algorithm. Table 5.3 shows all the hop time estimation results.

SNR	**1%**	**5%**	**10%**	**15%**	**20%**	**30%**	**40%**	**50%**
15	0.796	0.966	0.9800	0.9840	0.9840	1	1	1
10	0.676	0.906	0.926	0.932	0.938	0.944	0.946	0.946
6	0.474	0.812	0.848	0.868	0.884	0.898	0.898	0.904
3	0.35	0.71	0.77	0.816	0.836	0.874	0.9	0.904
0	0.122	0.34	0.48	0.594	0.682	0.78	0.832	0.872
-3	0.086	0.154	0.252	0.33	0.398	0.456	0.498	0.526

Table 5.3 Hop Time Estimation Results showing probabilities of estimated hops having a given distance, represented as percentage of T_{hop_min} from true hop time

In the table 5.3, column labeled 1% indicates the probability of the detected hops having an estimated hop time within 1% of T_{hop_min} (256 sample points). 1% of T_{hop_min} means within 2 samples of the true hop time. Sampling is done at a frequency of 60 MHz, so one sample corresponds to 16.67 ns. For an SNR of 6 dB, the column labeled 1% indicates that estimated hop time of 47.4% of the detected hops is within 2 samples of the actual hop time. Similarly the column labeled 5% indicates that the estimated hop time of 81.2% of the detected hops is within 12 samples of the true hop time.

Figure 5.2 shows the accuracy of hop time estimation in terms of probabilities.

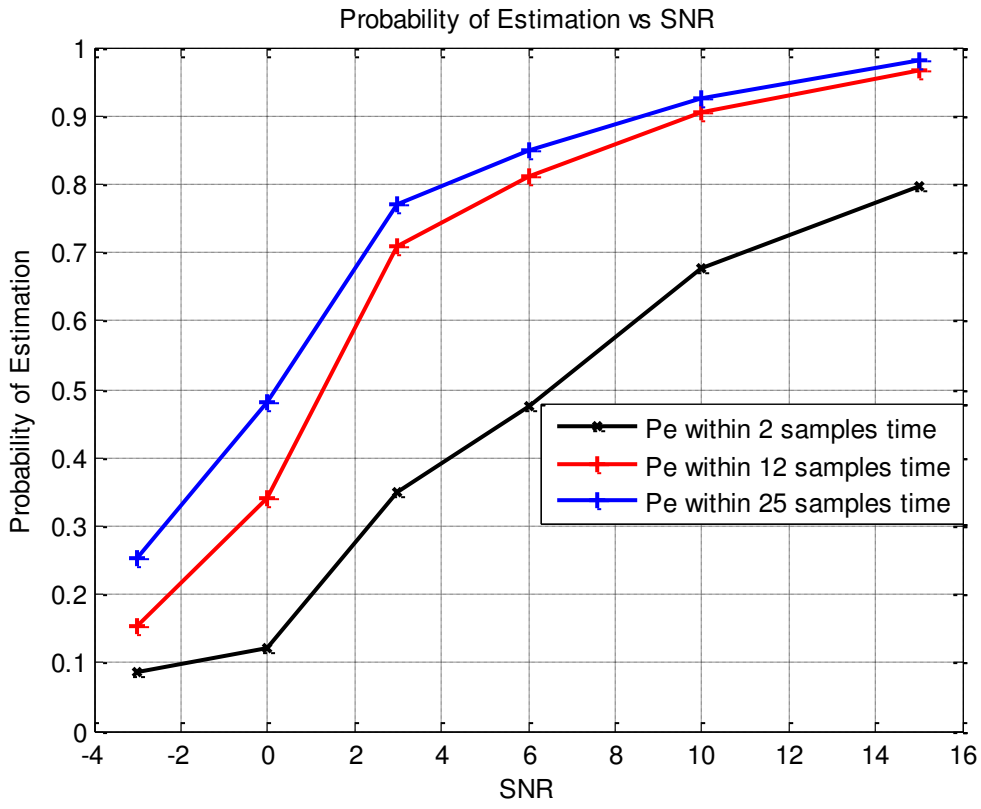

Figure 5.2 Probability of Estimation vs SNR

It can be observed from the figure that with an increase in SNR, the probability of hop time estimation within a given number of samples time also increases. The lowest plot in

the figure corresponds to the probability of detected hops having estimated hop time within 1% (2 samples time i.e.33.34 ns). The middle plot corresponds to the probability of detected hops having estimated hop time within 5% (12 samples time i.e. 0.2 μs) and the uppermost plot corresponds to the probability of detected hops having estimated hop time within 10% (25 samples time i.e. 0.417 μs).

Chapter 6

CONCLUSIONS AND RECOMMENDATIONS FOR FUTURE WORK

6.1 Conclusions

The thesis is based on the application of Temporal Correlation Function and Discrete Wavelet Transform for the Detection and Hop time Estimation of a Frequency Hopping Signal in HF band (2 – 30 MHz) in Additive White Gaussian Noise. HF band is specifically used for military applications for security purposes.

An introduction of Frequency Hopping Spread Spectrum technique is provided. After that an analytic expression of a FH signal is derived. A two-dimensional Temporal Correlation Function of the analytic FH signal is computed. The phase of the TCF expression is plotted and the phase discontinuities are enhanced by pre-processing and most importantly, by applying the Discrete Wavelet Transform. The Detection and Hop Time Estimation Algorithm "Detects" the presence or absence of a hop in the frame. It further estimates the time of hop.

Results show acceptable detection performance at SNR levels above 3 dB. At 3 dB probability of detection is 0.96 with 8.6% misclassification. Hop time estimation accuracy is also reliable at SNR levels above 3 dB.

6.2 Future Work

The work is based on the two-dimensional plot of the phase of Temporal Correlation Function. The results can be improved by applying image processing techniques for de-noising and for enhancing the hop time estimation accuracy. Morphological image

processing techniques can be applied to the phase plot of Temporal Correlation Function. Wavelet based two-dimensional edge detection technique can be utilized to refine the detection and hop time estimation results even at SNR levels lower than 3 dB.

BIBLIOGRAPHY

[1] W. J. L. Read, "Detection of frequency hopping signals in digital wideband data," tech. rep., Defense Research and Development Canada, December 2002.

[2] K. Jaiswal, "Spectral sensing of adaptive frequency hopping signal for cognitive radio," in Proceedings of the IEEE International Conference on Performance, Computing and Communications, pp. 360-365, December 2008.

[3] T.C.Chen, “Joint signal parameter estimation of frequency hopping Communications”, IET Communications, August 2011

[4] Fan, H., Guo, Y., Feng, X. “Blind parameter estimation of frequency hopping signals based on matching pursuit”, Wireless Information Communication, 2008

[5] D. Torrieri. “Principles of Spread-Spectrum Communication Systems”, Springer, second edition, 2011.

[6] Y-P. Cheng, “Detection of Frequency Hopped Signals Timing Information Using The Temporal Correlation Function”, MS Thesis, Monterey, California, Naval Postgraduate School, 2008

[7] H. F. Overdyk, Detection And Estimation of Frequency Hopping Signals Using Wavelet Transforms, MS Thesis, Naval Postgraduate School, Sep. 1997.

[8] J.Miček, J.Kapitulík, “Median Filter”, Journal of Information, Control and Management Systems, Vol. 1, (2003)

[9] O. Rioul, M. Vetterli, “Wavelets and signal processing”, IEEE Signal Processing Magazine, Vol. 8, Oct. 1991, pp.14 – 38.

[10] C.Valens, “A Really Friendly Guide to Wavelets”, Tutorial, 1999

[11] Gonzalez, R.E. Woods, “Digital Image Processing”, Second Edition 2002

[12] M. Sirotiya and A. Banerjee, “Detection and Estimation of Frequency Hopping Signals Using Wavelet Transform,” Cognitive Wireless Systems (UKIWCWS), 2010 Second UK-India-IDRC International Workshop on, pp. 1-5, IEEE, 2010

[13] N. Shaik, K. O. Saravanan, H. Iqbal, “Compressive Sensing Detection method for Frequency Hopping Signals”, International Journal of Advanced Trends in Computer Science and Engineering, 2014, Vol. 3 , No.1, Pages : 546– 548

[14] F. Lieu, “Compressive Measurement of Spread Spectrum Signals”, PhD Thesis, University of Arizona, Dec 2014

[15] J. Wu, N. Liu, Y. Zhang, C. Shen, “Blind Detection of Frequency Hopping Signal Based On Compressive Sensing”, IEEE, 2012

[16] F.Haining, G. Ying, X. Yaohua, “A Novel Algorithm of Blind Detection of Frequency Hopping Signal Based on Second-Order Cyclostationarit”, IEEE Congress on Image and Signal Processing, 2008